Development of a non-invasive evaluation methodology using a smartphone attachment on the diagnosis and follow-up of anemia

by

Berfin Irmak Torun

A Dissertation Submitted to the
Graduate School of Sciences and Engineering
in Partial Fulfillment of the Requirements for
the Degree of

Master of Science

in

(Biomedical Science and Engineering)

September 2, 2022

Development of a non-invasive evaluation methodology using a smartphone attachment on the diagnosis and follow-up of anemia

Koç University

Graduate School of Sciences and Engineering

This is to certify that I have examined this copy of a master's thesis by

Berfin Irmak Torun

and have found that it is complete and satisfactory in all respects,
and that any and all revisions required by the final
examining committee have been made.

Committee Members:

Özlem Yalçın, Prof. (Advisor)

Sacit Karamürsel, Prof.

Selçuk Tunalı, Prof.

Date: September 2, 2022

Dedicated to my family and my dearest friends

ABSTRACT

Anemia, which has multiple causes, such as iron deficiency, chronic blood loss, and hemolysis, is a prevalent health problem affecting an estimated two billion people or 30% of the world's population. The ability to measure hemoglobin concentration in anemic patients noninvasively and continuously has significant potential to facilitate hemoglobin monitoring, improve the detection of acute anemia, and avoid complications, expenses, and pain associated with invasive blood draws. Although some non-invasive approaches have been developed, they are less accurate than invasive methods as a clinical purpose, resulting in an unmet need for more accurate non-invasive methods.

In the present study, we conducted a feasibility study for a group of subjects who were admitted to Koc University Hospital, Hematology clinics and Lokman Hekim University Hematology and Internal Diseases clinics. Patients with the symptoms of anemia and healthy subjects who were scheduled to have their complete blood count (CBC) parameters measured with hematology blood analyzers as part of their clinical care were recruited for this study. After the patient's blood was collected to conduct their CBCs, high-resolution images were taken of those patients' palm finger areas with a smartphone camera via dermatoscope attachments. By examining the color characteristics of the images, we developed an image processing methodology to correlate color characteristics in smartphone images of palm to hemoglobin concentration measured with the gold standard hemoglobin measurement system which is CBC the test. According to the results, our method gives significant predicted Hgb values. We observed that our results indicate a correlation between erythema index values and CBC hemoglobin levels.

The main contribution of this thesis is proving the linear relationship between color characteristics of digital images and hemoglobin concentration measured in the laboratory. Without any reflectance measurement, this non-invasive calculation methodology is useful for objective assessment of erythema index and therefore hemoglobin levels. With the proposed methodology, in future cost-effective non-invasive point-of-care system that enables users to make self-care anemia evaluation and screening, which would replace the conventional method of anemia detection by visual observation of palm pallor colors Furthermore, with the developments in cloud technology, the study results can be improved by increasing the number of samples. This can be done with a system that will allow people who have already had blood counts to add photos to the cloud. Sensitivity can be optimized with a deep learning algorithm, which will be developed based on the correlation found, and values that are much closer to the real hemoglobin results can be obtained. The outcomes of this project can improve health services offered to patients with related diseases / disorders by supporting diagnosis, and early identification of critical situations related to disease severity and therefore decrease the percentage of severe complications of the diseases. These, in turn, are expected to yield significant economic benefits to patients by better planning treatment and avoiding unnecessary treatment schemas. Apart from savings on patient expenses, these savings also encourage health care providers to deliver high-quality, coordinated care at lower costs.

ÖZETÇE

Demir eksikliği, kronik kan kaybı ve hemoliz gibi birden çok nedeni olan anemi, tahminen iki milyar insanı veya dünya nüfusunun %30'unu etkileyen yaygın bir sağlık sorunudur. Anemik hastalarda hemoglobin konsantrasyonunu noninvaziv ve sürekli olarak ölçmek, hemoglobin değerini takip etmeyi kolaylaştırmak, akut aneminin saptanmasını iyileştirmek ve invaziv kan alımlarıyla ilişkili komplikasyonları, masrafları ve ağrıyı önlemek için önemli bir potansiyele sahiptir. Bugüne kadar bazı non-invaziv yaklaşımlar geliştirilmiş olsa da, klinik olarak invaziv yöntemlerden daha iyi sonuç vermemektedir. Bu durum doğruluğu daha fazla olan non-invaziv yöntemlere yönelik karşılanmamış bir ihtiyaç doğurur.

Bu çalışmada, Koç Üniversitesi Hastanesi, Hematoloji klinikleri ve Lokman Hekim Üniversitesi Hematoloji ve İç Hastalıkları kliniklerine başvuran bir grup hasta için fizibilite çalışması yaptık. Anemi semptomları olan hastalar ve klinik süreçlerinin bir parçası olarak tam kan sayımı (CBC) parametrelerinin ölçülmesini planlayan sağlıklı kişiler bu çalışmaya dahil edildi. Tam kan sayımlarını yapmak için hastalardan kan alındıktan sonra, bu hastaların avuç içi ve parmakbölgelerinin dermatoskop eklentisi aracılığıyla bir akıllı telefon kamerası ile yüksek çözünürlüklü görüntüleri alındı. Görüntülerin renk özelliklerini inceleyerek, avuç içi akıllı telefon görüntülerindeki renk özelliklerini, tam kan sayımı testi olan altın standart hemoglobin ölçüm sistemi ile ölçülen hemoglobin değeriyle ilişkilendirmek için bir görüntü işleme metodolojisi geliştirdik. Sonuçlara göre, yöntemimiz istitatiksel olarak tutarlı Hgb değerleri vermektedir. Sonuçlarımızın eritma indeks değerleri ile CBC hemoglobin seviyeleri arasında bir korelasyon gösterdiğini gözlemledik.

Bu tezin temel katkısı, dijital görüntülerin renk özellikleri ile laboratuvarda ölçülen hemoglobin konsantrasyonu arasındaki doğrusal ilişkiyi kanıtlamaktır. Herhangi bir reflektans ölçümü olmaksızın, bu non-invaziv hesaplama metodolojisi, eritma indeksinin ve dolayısıyla hemoglobin düzeylerinin objektif olarak değerlendirilmesi için faydalıdır. Önerilen metodoloji ile, gelecekte avuç içi renklerinin görsel olarak gözlemlenmesiyle geleneksel anemi saptama yönteminin yerini alacak, kullanıcıların kendi kendine anemi değerlendirmesi ve taraması yapmalarını sağlayan uygun maliyetli, invaziv olmayan bir ölçüm yöntemi geliştirebilmektedir. Aynı zamanda bulut teknolojisindeki gelişmelerle birlikte örneklem sayısı artırılarak çalışma sonuçları iyileştirilebilmektedir. Bu, daha önce kan sayımı yaptırmış kişilerin buluta fotoğraf eklemesine izin verecek birsistemle yapılabilir. Bulunan korelasyona göre geliştirilecek bir derin öğrenme algoritması ile hassasiyet optimize edilebilir ve gerçek hemoglobin sonuçlarına çok daha yakın değerler elde edilebilir. Bu projenin sonuçları, hastalığın ciddiyeti ile ilgili kritik durumların erken teşhisini ve erken teşhisini destekleyerek ilgili hastalıkları/bozuklukları olan hastalara sunulan sağlık hizmetlerini iyileştirebilir ve böylece hastalıkların komplikasyon yüzdesini azaltabilir. Bunların da tedaviyi daha iyi planlayarak ve gereksiz tedavi şemalarından kaçınarak hastalara önemli ekonomik faydalar sağlaması beklenmektedir. Hasta giderlerindeki tasarrufların yanı sıra, bu tasarruflar aynı zamanda sağlık hizmeti sağlayıcılarını daha düşük maliyetlerle, daha efektif ve planlı hasta bakımı sunmasını destekler.

AKNOWLEDGEMENTS

I have come to the end of my 4-year academic career at Koç University, where I first set foot as an intern in the fall of 2018. Ever since I was a child, I wanted to become a scientist. Today as I leave Koç University, I know that I have fulfilled this dream.

I would like to start by thanking my parents Füsun and Hüseyin Torun, who have provided every support that has helped me pursue my academic career. I am very grateful to them for continuing to believe in me no matter what. They raised an engineer and a scientist.

I would like to express my gratitude to my primary supervisor, Özlem Yalçın, who is an example to me of how a scientist should be in every sense. She did not just provide a mentorship to be but also, she showed me what it means to be a woman in STEM. I will be forever grateful for her guidance.

I also could not have undertaken this journey without my defence committee, Selçuk Tunalı, who has sparked my interest in research since my childhood. I will never forget the cadaver bones he gave me when I was 10 years old to use in a science project.

I would like to thank my colleagues in the AGS Medikal, Gonca Turna and Bige Varlıer, who supported me in continuing my thesis studies and helped me to create time between work and academic life.

Words cannot express my gratitude to my undergraduate advisor Prof. Osman Eroğul, who trusted and motivated me to study at Koç University.

I would like to thank my best friends Nursima Zengin and Beyza Ayaz, for their continued friendship, immeasurable support, and care. I wouldn't have gotten to where I am today without them. Their belief in me has kept my motivation high especially at the hardest times of my academic life.

I am also grateful for the doctors and professors in both Koç University Hospital and Lokman Hekim University Hospital who sacrificed their time and offered their support to help me through this project.

Finally, I would be remiss in not mentioning my dearest friend İlayda Terzi, for keeping me connected to the academy and Koç University after I started working in the medical field.

TABLE OF CONTENTS

LIST OF TABLES

LIST OF FIGURES

ABBREVIATIONS

ACD	Anemia with Chronic Disorders
CA	California
CBC	Complete Blood Count
CCD	Charge Coupled Device
CI	Confidence Interval
COVID-19	Coronavirus Disease 2019
DIFF	Differential Leukocyte Count
EI	Erythema Index
Hb	Hemoglobin
HCT	Hematocrit
HGB	Hemoglobin
IDA	Iron Deficiency Anemia
IRB	Institutional Review Board
JPEG	Joint Photographic Experts Group
LIR	Laser Induced Reactions
MCH	Mean Cell Hemoglobin
MCV	Mean Corpuscular Volume
MDS	Myelodysplastic Syndrome
NIR	Near Infrared
POC	Point of Care
PPG	Photoplethysmography
RBC	Red Blood Cell Count
RDW	Red Cell Distribution Width
RGB	Red Green Blue
ROI	Region of Interest
RPI	Reticulocyte Production Index
SARS-Cov-2	Severe Acute Respiratory Syndrome Coronavirus 2
TIBC	Total Iron Binding Capacity
USA	United States of America
UVR	Ultraviolet Radiation

WA	Washington
WHO	World Health Organization

Chapter 1: **INTRODUCTION**

Anemia is a type of blood condition in which the concentration of hemoglobin or the number of red blood cells is inadequate to fulfill the physiological needs of the body. [1] Anemia is a prevalent health problem affecting an estimated two billion people or 30% of the world's population [2] and it leads to increased morbidity and mortality, diminished productivity at work, and impaired neurological growth. [3] Children, particularly infants, [4] women of productive age, pregnant women [5], and elders, as the risk of anemia in adults over 50 years of age increases with age, are the population groups that most vulnerable to anemia. [6] Although iron deficiency is globally the most common cause, anemia has multiple causes, such as nutritional deficiencies, parasitic infections, acute and chronic inflammation, malaria, [7] genetic hemoglobin disorders that affect the synthesis of hemoglobin or the production of red blood cells and hemolysis. [1]

To define anemia, the hemoglobin concentration is the most accepted hematological assessment methodology. [8] The detrimental effects on health and growth outcomes of anemia are attributed to the effects of reduced supply of oxygen to tissues as well as to the underlying causes of anemia. [3] The most prevalent clinical manifestations of anemia, including fatigue, dyspnea, tachycardia, and conjunctival and palmar pallor, can be explained by the role of hemoglobin in delivering oxygen to the tissues. [9]

Anemia is very common among infants and adolescents especially in developed countries [10], and it is associated with negative health and development outcomes, including neonatal and perinatal mortality, reduced physical growth, and impaired cognitive development. [11] Due to its detrimental effects on infant and child morbidity and mortality, especially when it coexists with malnutrition [12], anemia is seen as a measure of nutritional and health status in children. [13] The anamnesis and physical examination of the patient such as assessment of palmar pallor as the primary evaluation tool, are recommended [13] when the laboratory diagnosis of anemia or hematological data are unavailable and unaffordable to use especially in developed countries. [15]

The ability to measure hemoglobin concentration in anemic patients is necessary to make a prompt and accurate diagnosis and to initiate proactive steps to reduce the negative effects of anemia. [15] The golden standard for hemoglobin measurement is based on analysis on routine hematological tests such as CBC (complete blood count) and reticulocyte counts by hematology blood analyzers using a blood sample and this hemoglobin measurement technique still in use because of its reliability and consistency. [16] However, laboratory hemoglobin concentration measurements are relatively time-consuming, painful, due to invasive blood draws, and have a significant associated cost which can create an issue to access proper diagnosis and treatment in developing countries where anemia is most prevalent. It is therefore important to diagnose anemia non-invasively and continuously has a major potential to enhance hemoglobin monitoring, improve the diagnosis of acute anemia, and prevent complications, expense, and discomfort associated with invasive blood draws. [17]

There is growing interest and research into non-invasive approaches in the evaluation of health parameters. Patients prefer non-invasive diagnostic tests due to their accessibility, versatility, portability, and low-cost. Several methods have been developed to detect hemoglobin levels non-invasively including point-of-care devices, spectrum-based techniques, and smartphone-based approaches, although they are less accurate than invasive methods as a clinical purpose, resulting in an unmet need for more accurate non-invasive methods.

Classification of Anemia

Anemia is divided into three types based on its pathogenesis, red cell morphology, and clinical manifestation. Anemia can be classified by identifying acute blood loss according to the form of clinical presentation. [**?**] For clinical approaches, classification based on mean corpuscular volume (MCV) which is one of red cell morphology parameters, enables for a faster diagnose. Therefore, anemia can be divided into three types: microcytic, normocytic, or macrocytic, depending on MCV. On the other hand, based on pathogenic mechanisms anemia can be classified as hypo-regenerative or regenerative by reticulocytes count. Most automated hematological cell counters can provide both parameters on a regular basis. [18]

After identifying the presence of acute blood loss, isolated anemia should be distinguished from pancytopenia which is a condition that occurs when person has low counts of all three types of blood cells [19] by checking complete blood count and platelets. Patients who have isolated anemia should be evaluated whether it caused by decrease in red blood cell production (underproduction) or increase in red blood cell destruction (hemolysis), according to their reticulocyte production index. [20] Following that, diagnostic criteria can be based on either morphologic or pathophysiologic. The calculation of reticulocyte production index (RPI): RPI = correcteds reticulocyte count (%) × (haematocrit observed/normal hematocrit): F (reticulocyte maturation times in vivo). A reticulocyte production index greater than 2.5 suggests that hemolysis is likely which proves the bone marrow shows a normal regenerative capacity (regenerative anemia). [21] If reticulocyte production index less than 2 or 2.5 it indicates that there is a problem in production of anemia which shows that the bone marrow does not have regenerative capacity (hypo-regenerative anemia). [18]

Underproduction anemia or hypo-regenerative anemia morphologically, can be classified into microcytic (MCV, <80 fL), normocytic (MCV, 80-100 fL), or macrocytic (MCV, >100 fL) due to MCV [22] values and it is caused by changes in bone marrow progenitor cells. It is important to note that MCV is an average value and therefore does not provide details about the homogeneity of the erythrocyte population. [18]
When dealing with microcytic anemia, the most common diagnoses are iron deficiency anemia (IDA), thalassemia, anemia with chronic disorders (ACD), and sideroblastic anemia. [23] The most common cause of anemia is iron deficiency. Therefore, it is important to determination of the serum ferritin level and the levels of other iron metabolism parameters such as serum iron, total transport capacity of iron, and transferrin as the initial steps for all patients with microcytic anemia. [24] If the serum ferritin level and the other iron metabolism parameters levels are normal it should be considered whether the microcytosis is acute or chronic. A diagnosis of thalassemia should be considered in patients with chronic microcytosis. The analysis by Hgb electrophoresis can gives a diagnosis of thalassemia however, it does not always detect the presence of thalassemia. [25]

The central issue in normocytic anemia is identifying the causes including bleeding, nutritional anemia, anemia of renal insufficiency, anemia of chronic disease or

primary bone marrow suppression (aplastic anemia, leukemia). Iron, vitamin B12 and folate deficiencies are possible causes of nutritional anemia. If nutritional anemia is not the case, determining serum creatinine level or bone marrow biopsy can be helpful to address the cause easily. [25]

Macrocytic anemia can be divided into two subgroups due to nucleic acid metabolism as megaloblastic or non-megaloblastic. In the absence of drug or alcohol use, the most common cause of microcytic anemia is nutritional deficiency. When megaloblastic anemia mostly caused by nutritional deficiencies, non-megaloblastic anemia can be caused by liver dysfunction, alcoholism, myelodysplastic syndrome (MDS), or hypothyroidism. [26]

Hemolysis is a disorder in which red blood cells breakdown in circulation, causing hemolytic anemia. [27] Hemolysis, can be intrinsic (acute) or extrinsic (chronic). Hemolysis is classified in a variety of ways including autoimmune hemolytic anemia, alloimmune, drug induced, hemoglobinopathy and microangiopathic hemolytic anemia. [28]

Laboratory Approaches to Anemia

Although, the anamnesis and physical examination can suggest the existence of anemia, for current technologic methods, laboratory assessment is necessary for accurate diagnosis and treatment. [29] Evaluation of complete blood count (CBC) measurements is the gold standard for anemia diagnose. [30] A complete blood count includes hemoglobin, hematocrit, and red cell indices which are the mean cell volume (MCV], mean cell hemoglobin (MCH), mean concentration of hemoglobin per volume of red cells. Additionally, other tests for diagnosis of anemia are done with routine complete blood count test such as reticulocyte count and studies of iron status including serum iron, total iron binding capacity (TIBC) and serum ferritin. [31] Differential leukocyte count (DIFF) is also commonly performed after complete blood count test; however, both tests can currently be performed by automated hematology analyzers. [32] In some circumstances, a microscopic analysis of a blood smear is required. There are three types of blood smear examination including blood smear scan, blood smear examination, and blood smear review, all done by a knowledgeable laboratory professional. [33]

1.1 Non-Invasive Anemia Evaluation Methodologies

Visual inspection of conjunctival pallor, nail beds, lips, tongue, and oral mucosa enable clinicians to detect anemia in general. However, further tests are mostly needed to confirm the diagnosis as most of these physical examinations may mislead the clinicians due to patients having different anatomical characteristics. At this point, blood tests through venipuncture comes into play which enables exact diagnosis of anemia. Although laboratory testing is currently the gold standard for quantitative hemoglobin (Hb) measurement, due to its invasive nature, it possesses several disadvantages and risks, including exposure of both the patients and healthcare workers to microorganisms that can cause infections through needles, the procedure being expensive due to use of machinery, delays in obtaining the results and the procedure being painful. All these handicaps resulted in the emerge of quicker, safer, and more cost-effective non-invasive methods for diagnosis of anemia.

1.1.1 Point of Care Systems

Point of care (POC) tools enable bedside Hb testing are especially useful in perioperative supervision and critical care to quickly assess a patient's Hb levels without requiring large sample volumes and expert training. POC tools available at home settings may also significantly increase the quality of life of home-bound patients and patients that require regular Hb monitoring, such as patients with chronic anemia, whose condition may rapidly deteriorate up to the point where they may require blood transfusions. To meet the demand for bedside Hb monitoring, the development of POC Hb measurement tools is essential, however, the applicability of POC applications is limited by constraints such as ease of use, speed, data integrity, reliability, and repeatability [34]. Other than semi non-invasive POC methodologies, pulse co-oximetry, occlusion spectroscopy, and transcutaneous reflection spectroscopy are methods that are used for non-invasive POC technologies. [65]

1.1.2 Optical Non-invasive Methods

Hemoglobin has optical properties such as absorption, transmission, and reflection in varying proportions depending on the wavelength of the photon. Non-invasive Hb estimation can also be done by using hemoglobin's optical characteristics. [42] There are several non-invasive optical methods for measuring the amount of Hgb and blood oxygenation levels in human tissue including photoplethysmography, fluorescence spectroscopy, blood oxygenation monitoring using continuous NIR spectrometry, ultraviolet and visible spectroscopies. [43] Hb is present in blood in a variety of forms, including Oxyhemoglobin (HbO2), Hemoglobin (Hb), Carboxyhemoglobin (HbCO), and Methemoglobin. [44] Oxyhemoglobin and hemoglobin are the most common types found in blood and they have different absorption characteristics. Hb forms absorb, transmit and scatter the light in wavelength. [45] The differences between absorption spectra of Hb and HbO2 led to development of optical methods. It is known that measuring the transmission or reflection of light through the blood volume can reveal pulsatile changes in blood volume in tissue and this technique is called photoplethysmography (PPG). [46] In this method an optical sensor system has been developed to measure real time Hb, SpO2 and pulse levels. Reflectance spectroscopy measures tissue's reflectance spectra and has been carried out by different studies. However, they present different challenges when monitoring Hb signals due to skin tissue absorption.

1.1.3 Smartphone Applications / Smartphone-Based Systems

Even though non-invasive nai and optical methods are widely available, their accuracy and reliability are still discussed and mostly the cost of the devices are high. Moreover, novel non-invasive and smartphone-based solutions have an advantage for Hb monitoring in the home setting and telehealth applications, as wellfor the comfort of the patients that may require frequent Hb measurements.
Smartphone-based solutions also have the advantage of storing the data in the cloud, which allows the healthcare provider to have access to chronological data on the patient's disease progression, as well as the ease of the integration of Hb values with other relevant medical data. As such, various studies that report novel non-invasive Hb quantification methods that use ordinary digital cameras or smartphones have been published.

1.1.4 Image Analysis Techniques for Detection of Anemia / Computer-Based Techniques

It has been known that patient's anamnesis and physical examination can suggest the existence of anemia and subjective measurement of pallor of the conjunctiva, nail beds, lips, and palms has commonly been used as a clinical sign. [57] Hb levels can be estimated using automated algorithms and they showed a high accuracy level. Although the region of interest was manually selected by the algorithms and fingers robustness could not be evaluated, using automated algorithms to analyse the colour of nail beds from smartphone pictures has been reported as a Hb estimated method. [58]

It has been postulated that, conjunctival color characteristics are linked to Hb concentration, and that digital representation of these characteristics is based on relative shades of red (R), green (G), and blue (B) [42] for each pixel and this point can be used to support the use of a color image processing technique for anemia detection. [61]

Chapter 2: **THEORETICAL BACKGROUND**

2.1 Physical Examination in The Diagnosis of Anemia

Prior to the development of modern health technology, physical examinations have been an important aspect of medical data collection for decades. [66] Even today, taking a patient's history and doing a physical examination are critical parts of the evaluation process. [67] For over three decades, it has been known that anemia can be assessed by examining the skin, nail beds, and conjunctiva. [68] However, the clinician's subjective assessment at the diagnosis stage, due to the nature of the physical evaluation, may question the accuracy of the result. [69] A possible solution is needed to eliminate this problem.

2.2 Erythema Index

Measurement of skin colour is useful in the assessment of some diseases and the degree of oxygenation of blood in the dermis and the existence of the epidermal pigment, melanin can determine the colour of healthy skin. [68]
Erythema is reddening of the skin caused by dilation of superficial blood vessels. In phototherapy and photochemotherapy, erythema is used to guide, anticipate, and adjust treatment strategies. [66] In the 1920s, Hausser and Vahle were the first to grade the degree of ultraviolet radiation-induced erythema. [67] The skin might become inflamed as a result of ultraviolet exposure. The erythema component of that response is frequently employed to assess the severity of skin damage or phototoxicity. They found that the formation of erythema in human skin by ultra-violet radiation is dependent on wavelength. [66]

Skin color can be measured using two methods: spectrophotometric and reflectance. [69] Despite our eyes' outstanding capacity to distinguish between colors, visual assessment of erythema is imprecise and subjective. For this, full-range, or narrow-band reflectance spectrophotometers and tristimulus colorimeters have been

used, especially for quantifying the erythema and pigmentation generated by UVR. [5] However, these devices were not handy when it comes to assessing smaller section then measuring area. After opto-electronic technology, such as CCD (charge coupled device) in video cameras, was developed, we were able to acquire photographs in which the color was replicated in a natural way. And we could be able to gather information from pixels of the images. Physicians performed experiments in the 1930s to validate and extend the findings. It has been known that skin reflectance can be used to diagnose erythema.

2.3 Optical Properties of Hemoglobin

Hemoglobin is one of the primary chromophores for visible light in the dermis and has optical properties such as absorption, transmission, and reflection in varying proportions depending on the wavelength of the photon. [42] Hb is present in blood in a variety of forms, including Oxyhemoglobin (HbO2), Hemoglobin (Hb), Carboxyhemoglobin (HbCO), and Methemoglobin. [44] Oxyhemoglobin and hemoglobin are the most common types found in blood and they have different absorption characteristics. Hb forms absorb, transmit and scatter the light in wavelength. [45] The differences between absorption spectra of oxyhemoglobin and hemoglobin led to development of optical hemoglobin estimation methods. In the spectral range 520-580 nm, oxyhaemoglobin shows high absorption of green light. Absorption in the red part of the visible spectrum decreases rapidly as wavelength increases, so absorption in the red part of the visible spectrum is low. [66] By comparing the amount of reflected red and green light, an index can be generated that is based primarily on the superficial dermis' blood content and this index is called erythema index.

2.4 Principles of Reflectance Spectroscopy

The absorption and scattering processes alter the light absorbed by tissue. Although the light that is scattered in the tissue affects all wavelengths that are determined by the probed sample, the light that is absorbed in the body at specific

wavelengths that are determined by the biochemical composition of the probed tissue. These two differences between absorption and scattering, enable us to evaluate the health of tissues. While the scattering of light provides the structural knowledge of the tissue, with analyzing the wavelength of reflected light tissue absorption information can be achieved.

The Beer-Lambert law of exponential attenuation with photon path length is used to describe tissue absorption. Like we mentioned before, hemoglobin is the most common tissue absorber and has different absorption spectrum among its forms. The degree to which each type of hemoglobin is absorbed provides information about their relative concentrations, as well as indirect information about tissue vascularity and metabolic status. This is the underlying principle of optical pulse oximeters, which use a simplified version of reflectance spectroscopy. [67]

2.5 Principle of operation of the early hemoglobin measurement systems

The technique of calculating the amount of green light re-emitted from the skin in vivo to measure erythema has been done before 1960s. [68] However, due to limitations in technology these methods were not efficient enough to use in clinic. In 80s researchers have used this technique to develop commercially available instruments. In 1980, J B Dawson et al developed a method to link the spectrum of light reflected from skin to the light absorbing from the skin. [69] For this they derivate a formula by making three assumptions including the optical properties of skin; Skin is composed of multiple layers, each transmits and scatters light similarly, formula which originally developed to explain diffuse reflectance of powders can be used describe the transmission and scattering of light by each layer and the light transmittance or reflectance of the system is unaffected by the interface between layers. The hemoglobin that found in the blood vessels of the upper dermis, is the main cutaneous chromophore of green light and reflectance spectrophotometry takes advantage of this fact. Their mathematical method is focused on reflectance spectroscopy's standard treatment. [70] And they demonstrated that cutaneous hemoglobin indices could be measured using measurements of light reflectance through skin at various wavelengths.

2.6 *Derivation of the formula*

The erythema index is calculated using Lambert-Beer's law and a multilayered skin model.

T represents the fraction of light incident on the surface that is transmitted by the layer

$$T = \frac{4b}{(1+\beta)^2 \exp(Kd) - (1-\beta)^2 \exp(-Kd)} \quad (0.1)$$

And R is the fraction of incident light that is diffusely reflected

$$R = \frac{(1-\beta)^2[\exp(Kd) - \exp(-Kd)]}{(1+\beta)^2 \exp(Kd) - (1-\beta)^2 \exp(-Kd)} \quad (0.2)$$

$$\beta = [k/(k+2s)]^{1/2} \; and \; K = [k + (k+2s)]^{1/2} \quad (0.3)$$

k represents the fraction of light absorbed per unit path length in the layer, s represents the fraction of light scattered per unit path length in the layer, and d represents the layer thickness.

There are two limiting conditions:

k >> s	T → exp(-Kd),	R → 0
k << s	T = 1/(1+sd),	R = sd/(1+sd)

(0.4)

The transmittance of a layer obeys the Beer-Lambert law of radiation absorption in the first case, when scattering within a layer is extremely small; in the second case, if sd >> 1, then T → 0 and R → 1 and this corresponds to a completely diffuse reflecting layer.

When applying this model to the LIR spectrum of skin, the first condition will be assumed to apply to the fibrous protein, melanin, and hemoglobin layers, and the second condition will be assumed to apply to the lowest (collagen/fat) layer. The

validity of this postulate was verified by subsequent experimental measurements. Where I_0 is the light intensity returning from a white diffuse reflector.

$$I = I_0(R_1 + T_1^2R_2 + T_1^2T_2^2R_3 + T_1^2T_2^2T_3^2R_4]$$

(0.5)

Reflectance spectrophotometry was used to analyze increasing thicknesses of connective tissue, and it was discovered that thicker layers of connective tissue reflected more strongly in the red region of the spectrum than thin layers. [5]

By assuming R_1, R_2, and R_3 << 1 in vivo, the proposed theoretical model can be extended to non-pigmented skin, and the reflectance (R) of the skin approximates:

$$R = \frac{I}{I_0} = T_1^2T_2^2T_3^2R_4$$

$$\log\left(\frac{1}{R}\right) = L$$

$$L = \log\left(\frac{Intensity\ of\ light\ reflected\ from\ white\ surface, I_0}{Intensity\ of\ light\ reflected\ from\ test\ surface, I}\right)$$

(0.6)

The following function demonstrates that by comparing the sum of reflected red and green light, an index can be calculated that is primarily dependent on the blood content of the superficial dermis:

$$Erythema\ index = log_{10}\left(\frac{Intensity\ of\ red\ component\ of\ reflected\ light}{Intensity\ of\ green\ component\ of\ reflected\ light}\right)$$

$$R_g \cong r + (1-r)(R_c + T_e^2R_d + T_e^2T_d^2R_s)$$

(0.7)

Where R_g is the reflectance of green light from skin, R_e and T_e are diffuse reflectance and transmittance of the epidermis, R_d and T_d are diffuse reflectance and transmittance of the dermis, and R_s is the are diffuse reflectance of the subcutaneous fat. By assuming r << 1, R_e << 1 and R_d << 1 in the case of photons with wavelengths spanning the visible spectrum:

$$R_g \cong T_e^2T_d^2R_s$$

$$T_d = 10^{-A/2}$$

(0.8)

Where A is a parameter that describes the blood absorbance in the subpapillary vascular plexus. We can obtain:

$$\log\left(\frac{1}{R_g}\right) = -\log(T_e^2) + A_g - \log(R_s)$$

(0.9)

Where R_r is the reflectance of red light measured at the same time we can obtain:

$$\log\left(\frac{1}{R_r}\right) = -\log(T_e^2) + A_r - \log(R_s)$$

(0.10)

We can calculate an erythema index by subtracting the logarithm of the inverse reflectance of red light from that of green light, which reduces the effect of epidermal melanin and light reflection from the tissue layer beneath the superficial plexus:

$$Erythema\ Index = \log\left(\frac{1}{R_g}\right) - \log\left(\frac{1}{R_r}\right) = \log\left(\frac{R_r}{R_g}\right) = \log(R_r) - \log(R_g)$$

(0.11)

Since R = W / S, where W is white standard and S indicates the brightness of the skin:

$$EI = \log\left(\frac{W_{green}}{S_{green)}}\right) - \log\left(\frac{W_{red}}{S_{red}}\right)$$

(0.12)

In white standard W_{green} and W_{red} is almost equal, therefore we can assume that:

$$EI = \log S_{red} - logS_{green}$$

(0.13)

Chapter 3: **IMAGEJ OPERATING PARAMETERS**

3.1 *Basics of Image J and pre-processing of images*

Image J is Java-based open-source public domain image processing and analyzing software. [71] Image J presents an interface that consists only of a menu bar that shows commands and toolbars. While commands in the menu bar are organized in different menus which consist of File, Edit, Image, Process, Analyze, Plugins, Window and Help, the toolbar enables selection, drawings and zooming etc. with different tools. Image J enables users to work on 8-bit, 16-bit and 32-bit images and different image formats. Figure 3:1 shows an example of Image J interface with additional window for the image. Colored images from patients in JPEG format can be displayed on the screen.

Images that are taken from the patients by smartphone camera are 32-bit, RGB images with JPEG (Joint Photographic Experts Group] format. Hence, these images can be split into 8-bit grayscale images which are red, green and blue elements of the original-colored images.

As it has been mentioned in Chapter 2, to calculate the EI, the logarithmic value of green should be subtracted from the logarithmic value of red. Based on this information, Split Channels command from Color submenu is used to create three 8-bit grayscale images which are the red, green, and blue components of the RGB image. As shown in Figure 3:2, to split images into red, green, and blue channels the processing step is Image -> Color -> Split Channels. Figure 3:3 demonstrates the result for the channel splitting process.

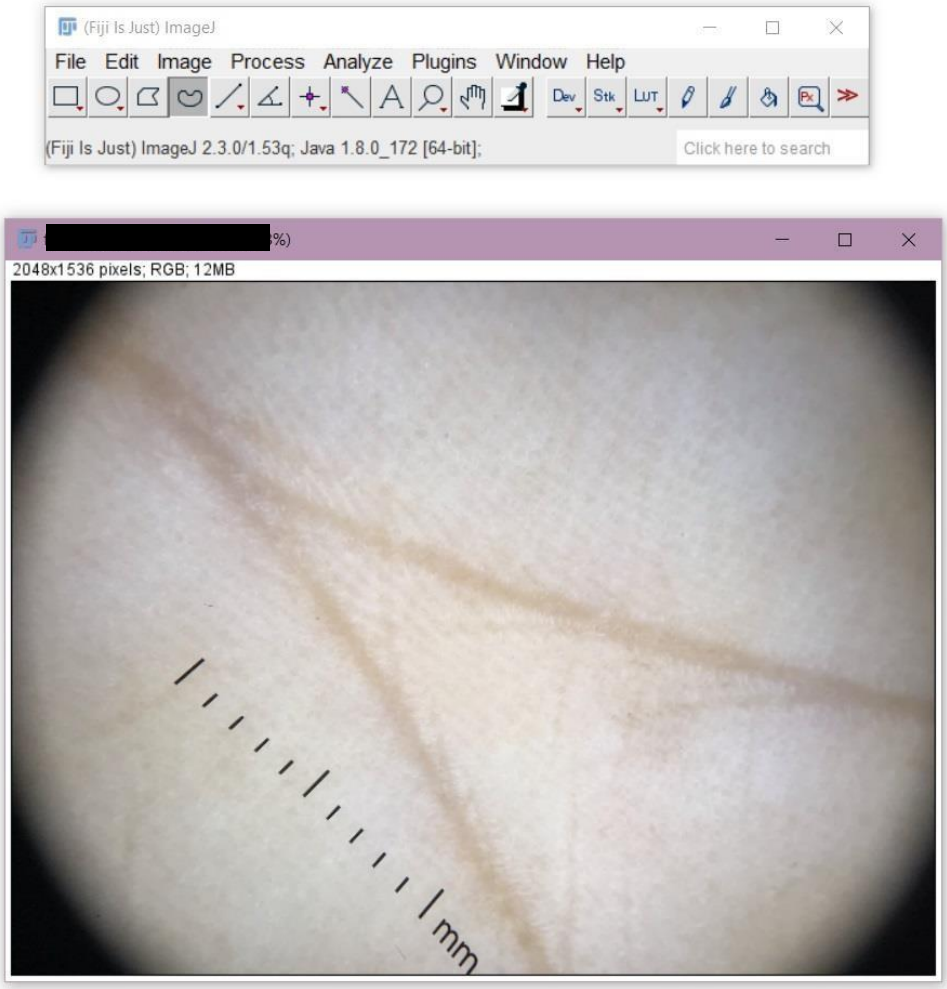

Figure 3.1 Image J interface

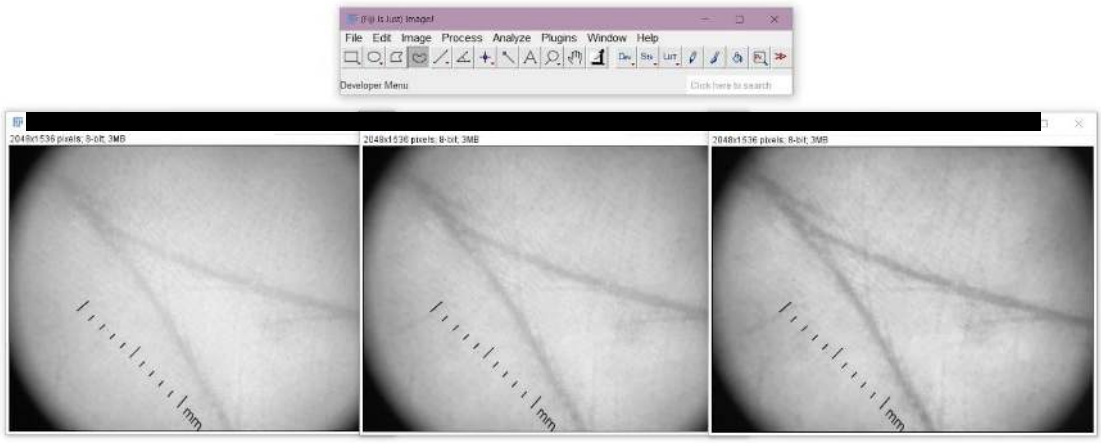

Figure 3.2 Image J Split Channels Result

From the formula of EI, it has been known that logarithmic values of red and green images should be taken before subtracting them from each other. As shown in the Figure 3:3, Process -> Math -> Log is the step for applying logarithm function into images. 8-bit red and green images have been changed due to use of function f(p) = ln(p) × 255 ⁄ ln (255) to each pixel (p). Figure 3:4 represents the results of logarithmic transformation on the images.

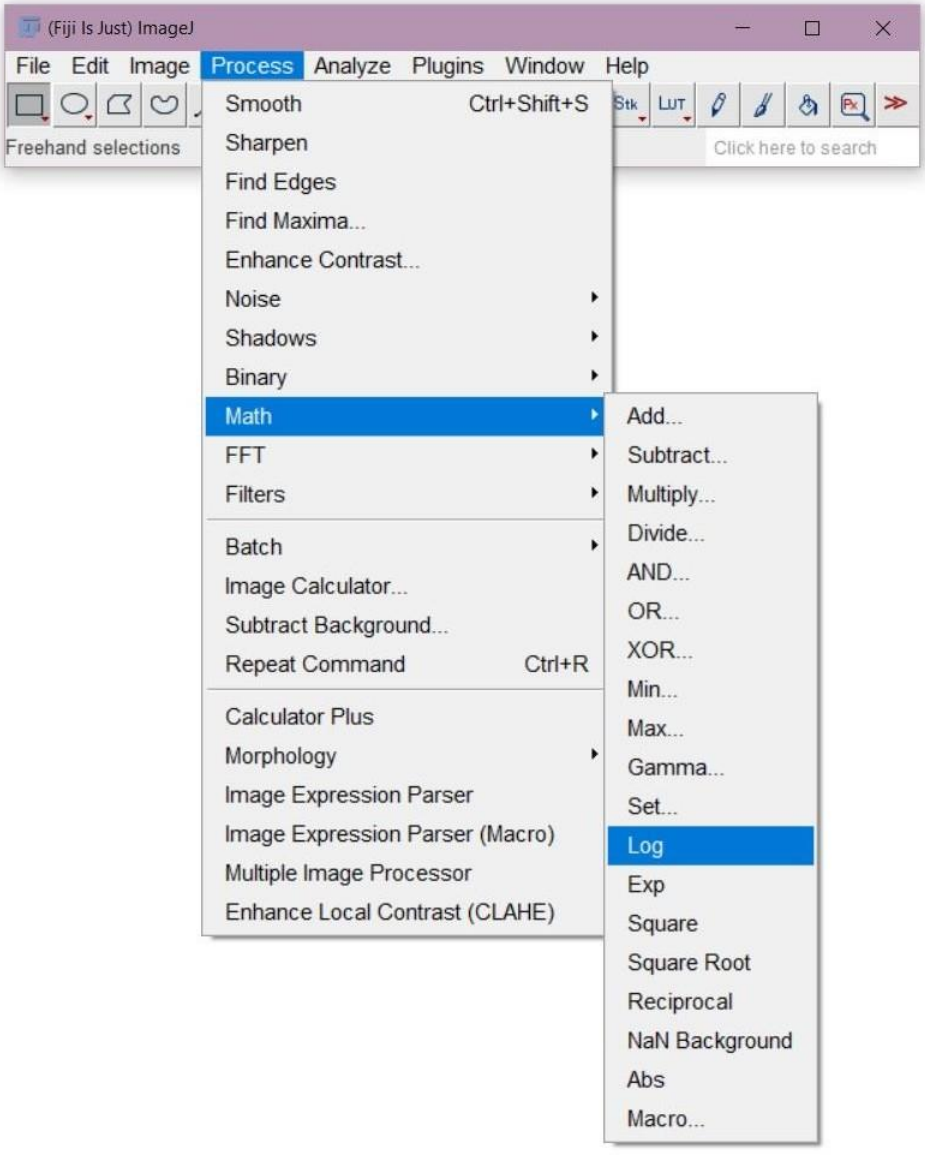

Figure 3.3 Applying logarithm function into images

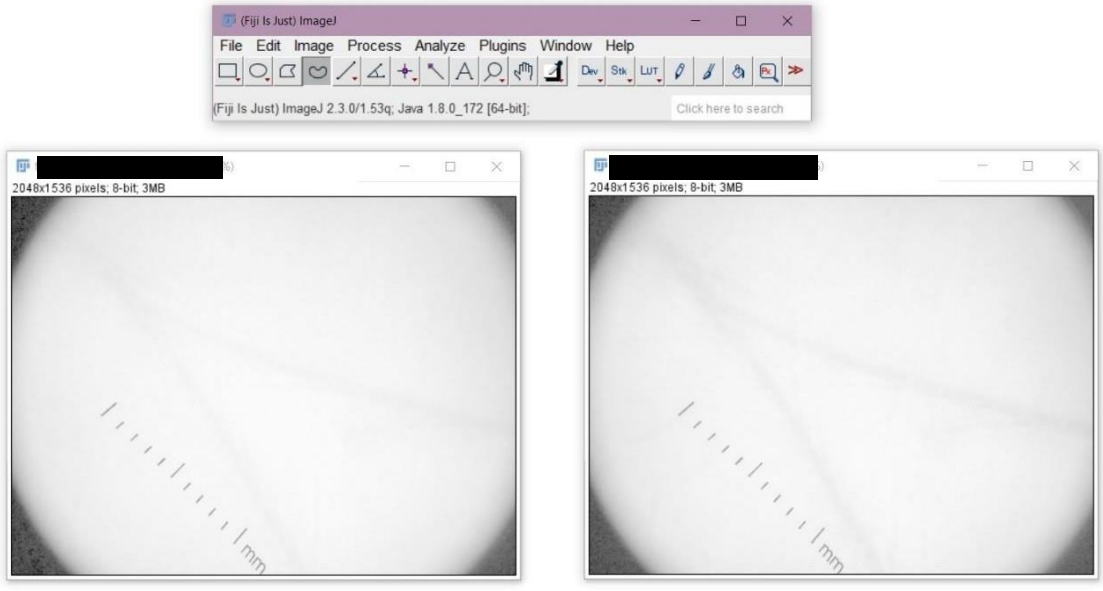

Figure 3.4 Results of logarithmic transformation on the images

After obtaining the results from logarithm command, according to the erythema index formula, the logarithmic result of the green image should be subtracted from the logarithmic result of the red image. As shown in the Figure 3:5, Process -> Image Calculator command creates a new window called Image Calculator and this section enables users to perform arithmetic and logical operations between two images. Figure 3:6 and Figure 3:7 display the Image Calculator window. To calculate the EI, Image1 should be chosen as the logarithmic result of the red image and Image2 should be chosen as the logarithmic result of the green image. As it mentioned before, the operation should be Subtract, due to the EI formula. Create New Window option should be checked to create a new image to hold the result.

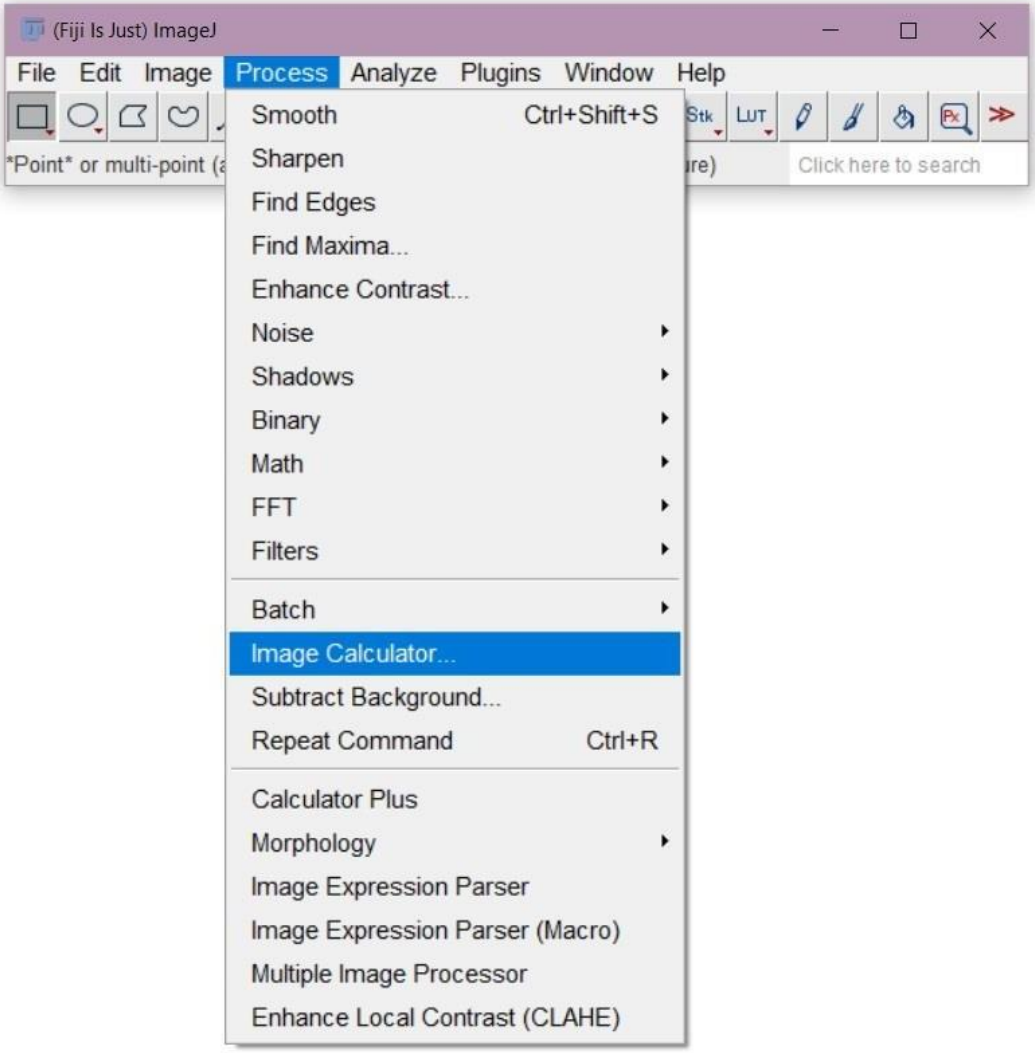

Figure 3.5 Image Calculator process

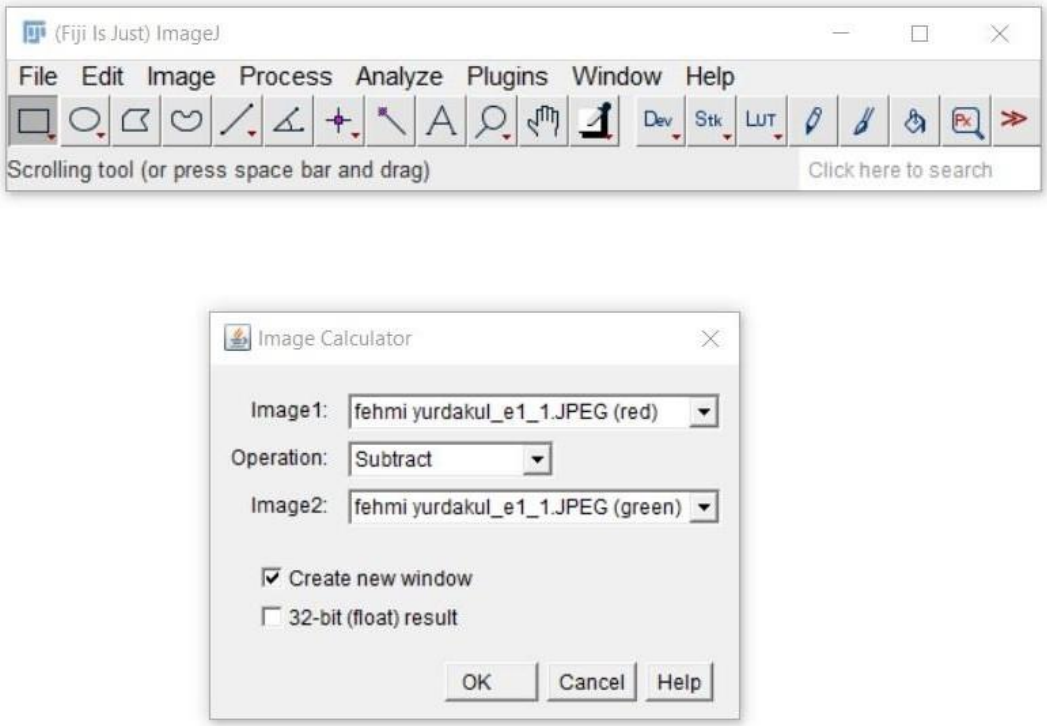

Figure 3.6 Image Calculator window

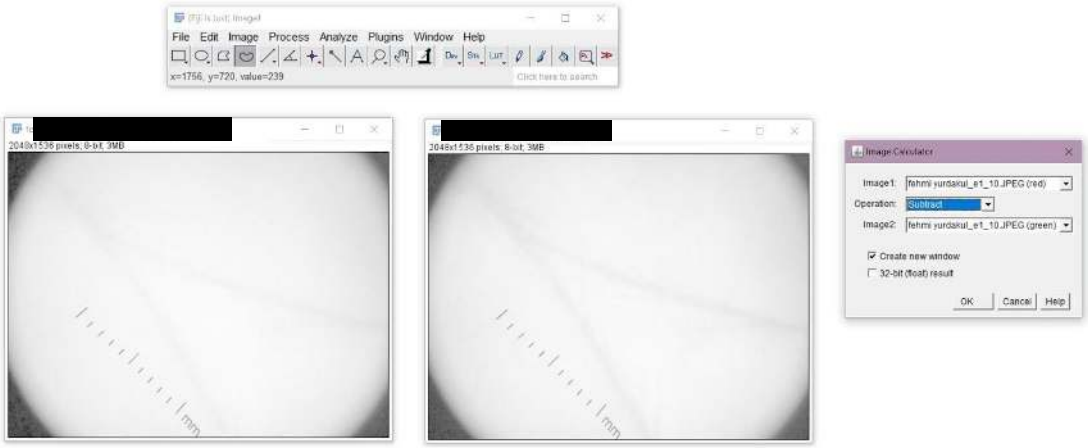

Figure 3.7 Images that will be subtracted from each other

Figure 3:8 shows the result of this image operation. Before necessary brightness adjustment, the image displays nearly as a black image. As shown in the Figure 3:9, Image -> Adjust -> Brightness/Contrast step allows to alter the brightness and contrast of the image with the B&C window which is displayed in Figure 3:10. For 8-bit images,

without modifying the pixel values, brightness and contrast of the image can be changed. The image's histogram is superimposed on a line graph at the top of the window that displays how pixel values are converted to 8-bit (0--255) display values. Based on an assessment of the image's histogram, Image J can also automatically adjust brightness and contrast. The image is optimized by allowing pixels to become saturated. The number of saturated pixels and hence the amount of optimization increases with each click on Auto. ImageJ shows pictures by linearly translating pixel values in the display range to values in the 0-255 range. Pixels that have less value than the minimum appear black, while those have more value than the maximum appear white. As the image appears almost black before the adjustment, the histogram plot shows pixel values around the point zero. With the Apply button, adjusted display range mapping function will be applied to the pixel data. Figure 3:11 and Figure 3:12 shows different brightness and contrast windows. While Figure 3:11 shows the histogram graph before clicking onto the Apply button, Figure 3:12 shows the applied version. The difference between both images emphasizes the alteration in the display range. Figure 3:13 represents the result of brightness and contrast adjustment.

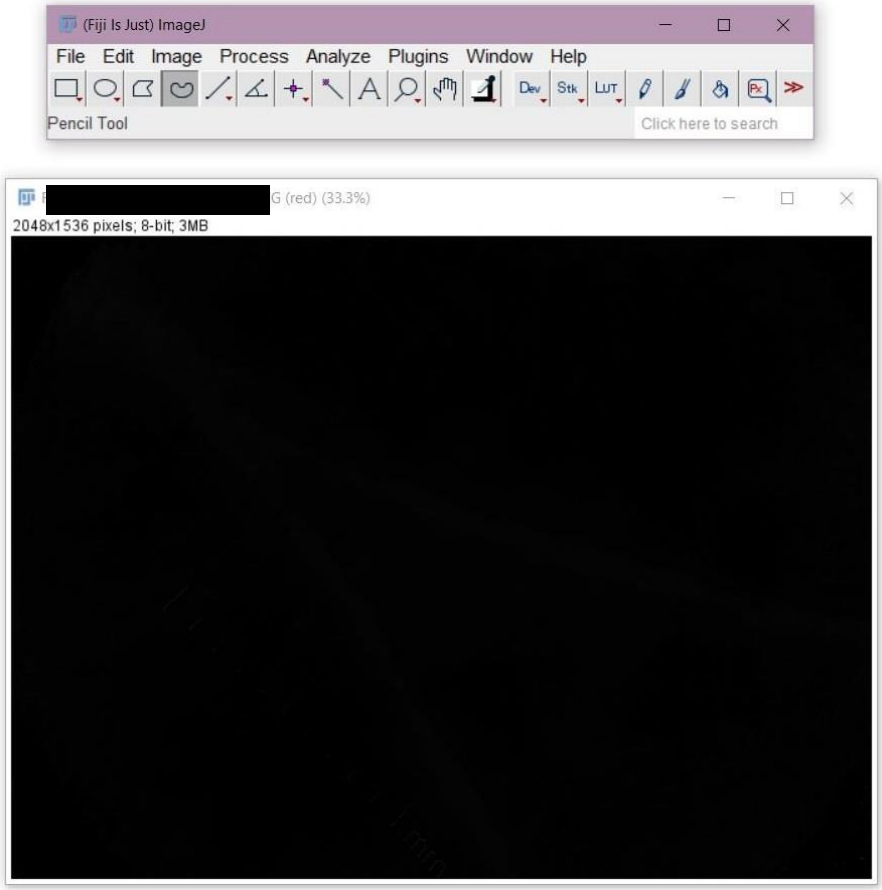

Figure 3.8 Result of Image Calculator command

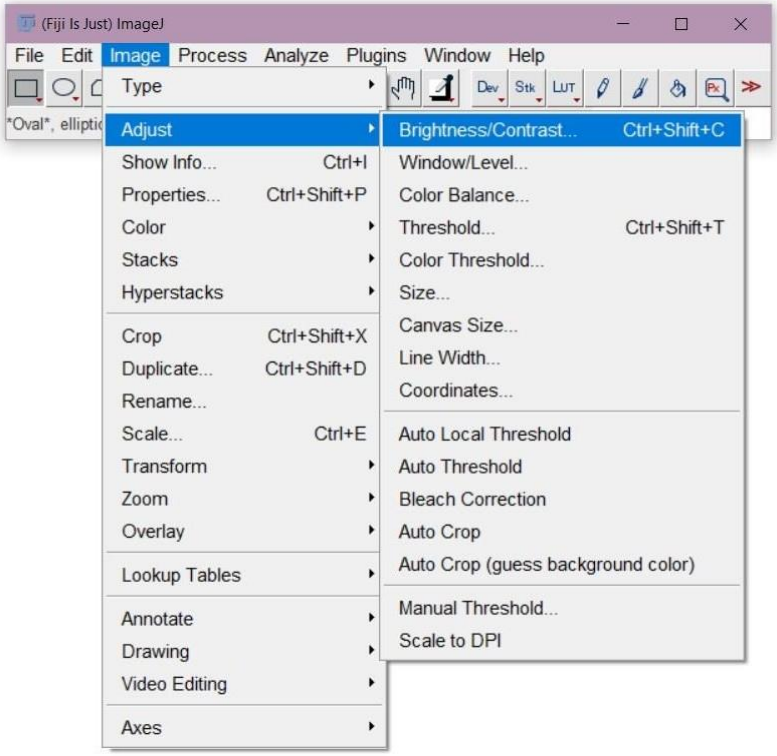

Figure 3.9 Steps of Brightness/Contrast adjustment

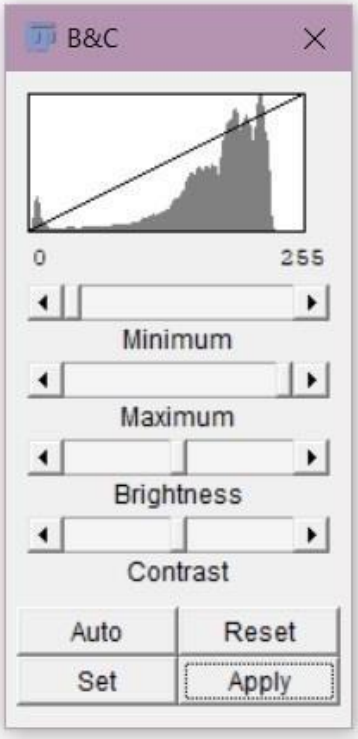

Figure 3.10 Brightness and Contrast window

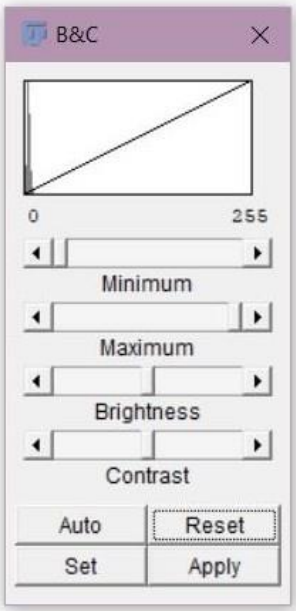

Figure 3.11 Brightness and Contrast window shows the histogram graph before clicking onto the Apply button

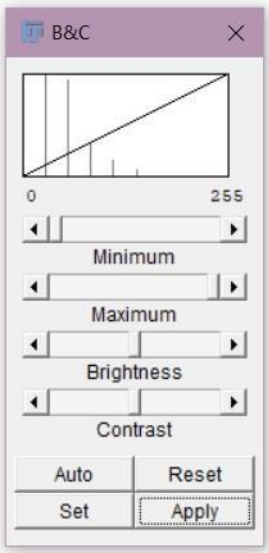

Figure 3.12 Brightness and Contrast window shows the histogram graph after clicking onto the Apply button

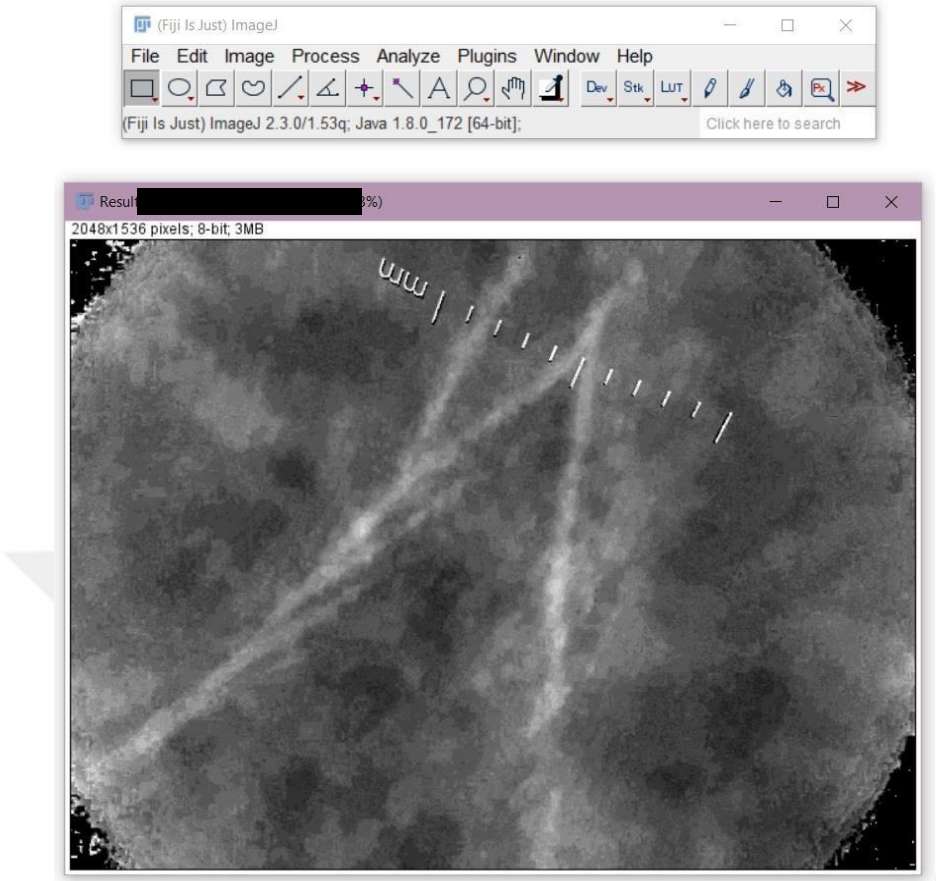

Figure 3.13 Result of Brightness and Contrast adjustment

Chapter 4: **ERYTHEMA INDEX ANALYSIS**

In this chapter, development of image analysis methodology to quantify the degree of erythema index is described. In this study, different regions of interest (ROI) have been applied to different body regions of interest to estimate the correlation between calculated erythema index and CBC hemoglobin value.

4.1 Region of interest (ROI) selection with ImageJ

After finishing the pre-processing part of the analyzing images that are taken from the patients with filter and mask procedures based on RGB color values in the pattern, to obtain an EI value it is necessary to define which subset of the images will be evaluated. Therefore, samples within the images should be selected as regions of interest (ROIs) for enhancing the precision level.

Main window of Image J contains a toolbar section to make different selections on the images. Figure 4:1 shows Image J tools in the toolbar. ImageJ has various tool selections to enable users to highlight different parts of the images to define specific regions of interest for every image.

To work on different ROIs, Image J enables users to manage multiple selections with the ROI (Region of Interest) Manager tool. While Figure 4:2 shows the step of Analyze -> Tool -> ROI Manager, Figure 4:3 displays the ROI Manager window. With clicking the Add button, the current selection will be added to the list. Users can update, delete, rename, measure, and make more different operations on the selected ROI. To use the Measure command, users should specify the measuring parameters from Analyze -> Set Measurements step in Figure 4:4 and Figure 4:5. In this study Mean gray value is chosen as a measurement parameter.

Figure 4.1 Image J Toolbar

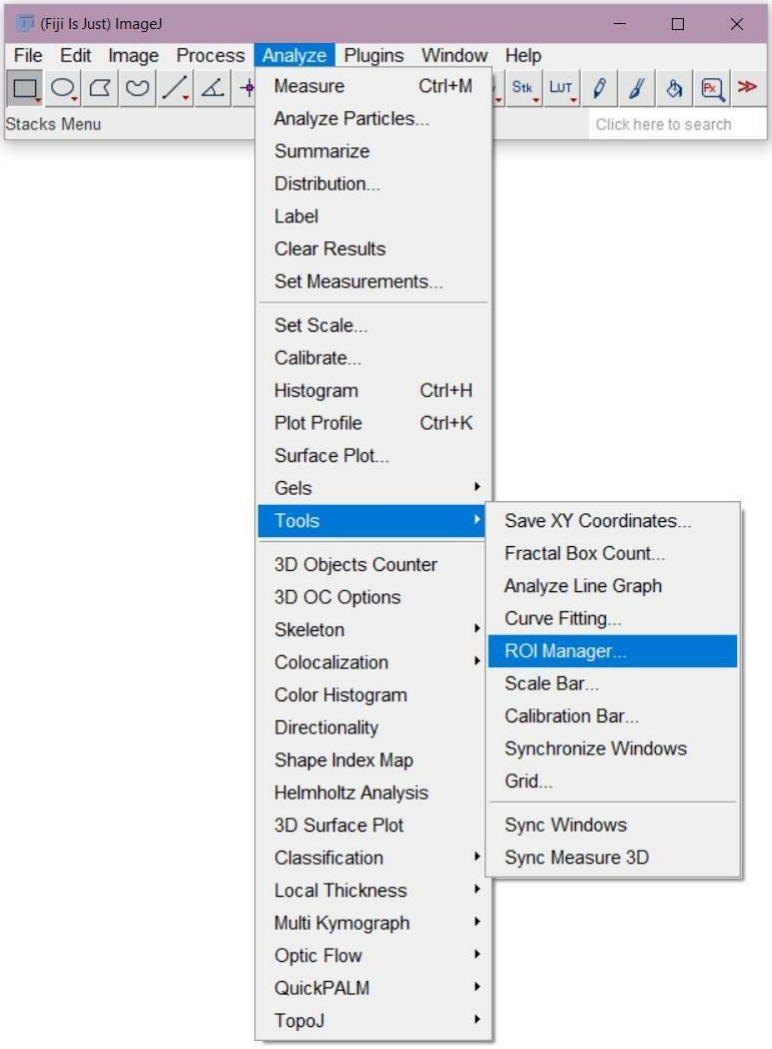

Figure 4.2 ROI Manager step

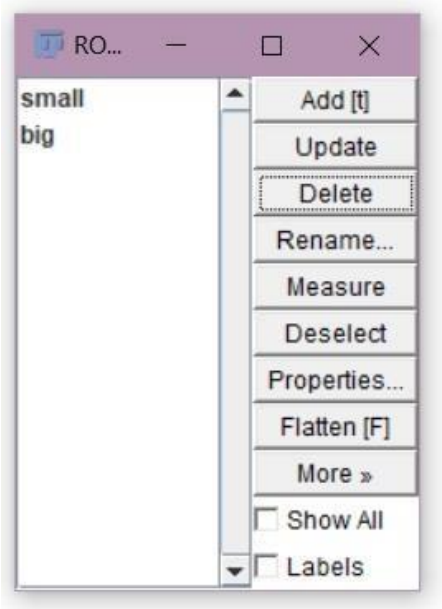

Figure 4.3 ROI Manager window

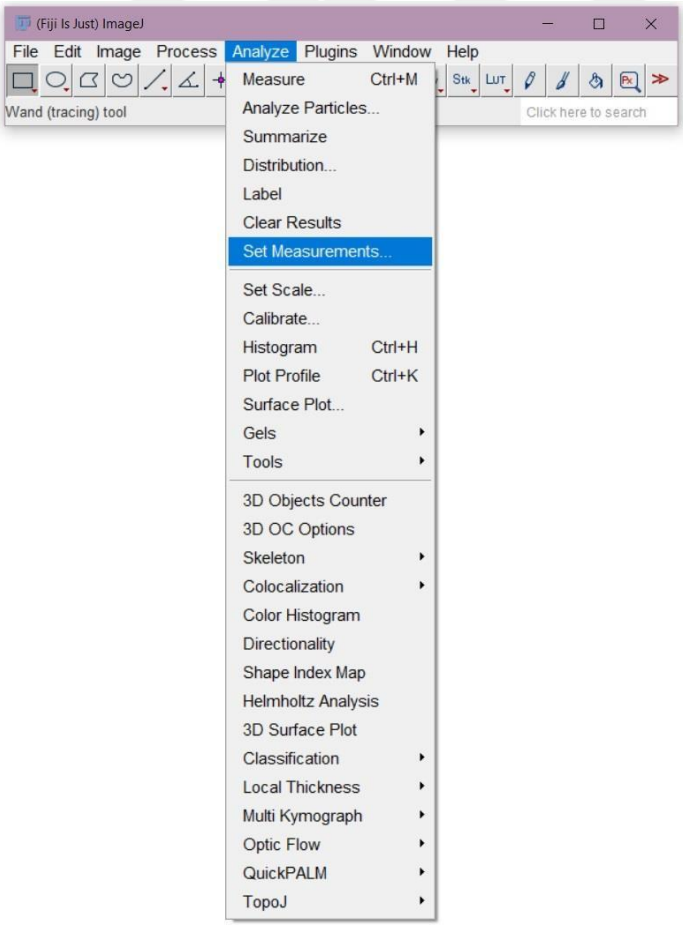

Figure 4.4 Set Measurements step

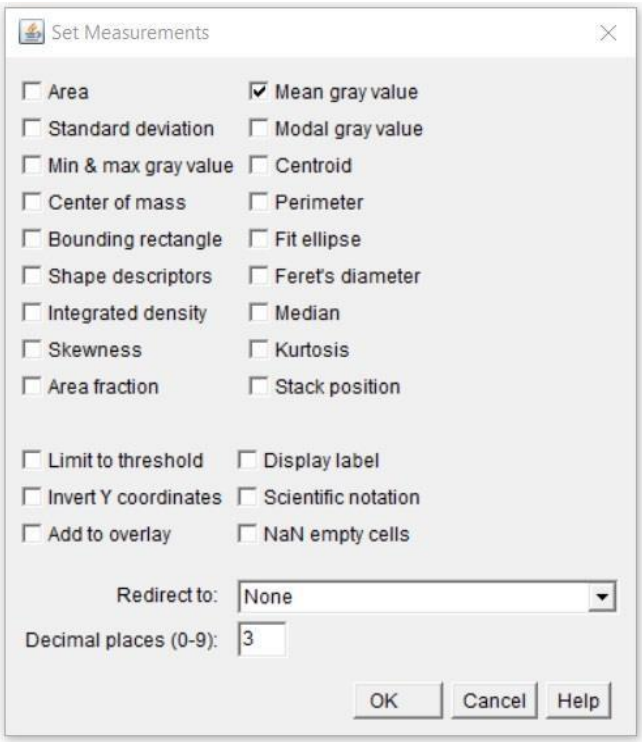

Figure 4.5 Set Measurements window

4.2 Determining the region of interests (ROIs)

In this study, Rectangular Selection Tool and Freehand Selection Tool are used to manually select different regions of interest to eliminate the limitation of automated region of interest selection.

As shown in Figure 4:6, two different ROIs are selected from each image with Rectangular Selection Tool. According to ROIs dimensions, the one with smaller dimensions is labeled as small and the other one which has bigger dimensions is labeled as big. To ensure the same selection of the ROI for different images, ROIs that are labeled as “small” and “big”, are standardized by fixing their dimensions to 400x400 pixels and 1000x1000 pixels respectively with Edit -> Selection -> Specify step. To validate the large dataset and eliminate the variation of images, the same type of ROIs which have the same dimensions were placed in every image manually. While Figure 4:7 shows the Specify command, Figure 4:8 and Figure 4:9 shows the adjustment of dimensions of small and big ROIs respectively.

Palm region images that are taken from the patients have similar features due to the structure of the palm. However, each palm has its own unique crease shapes and distribution.

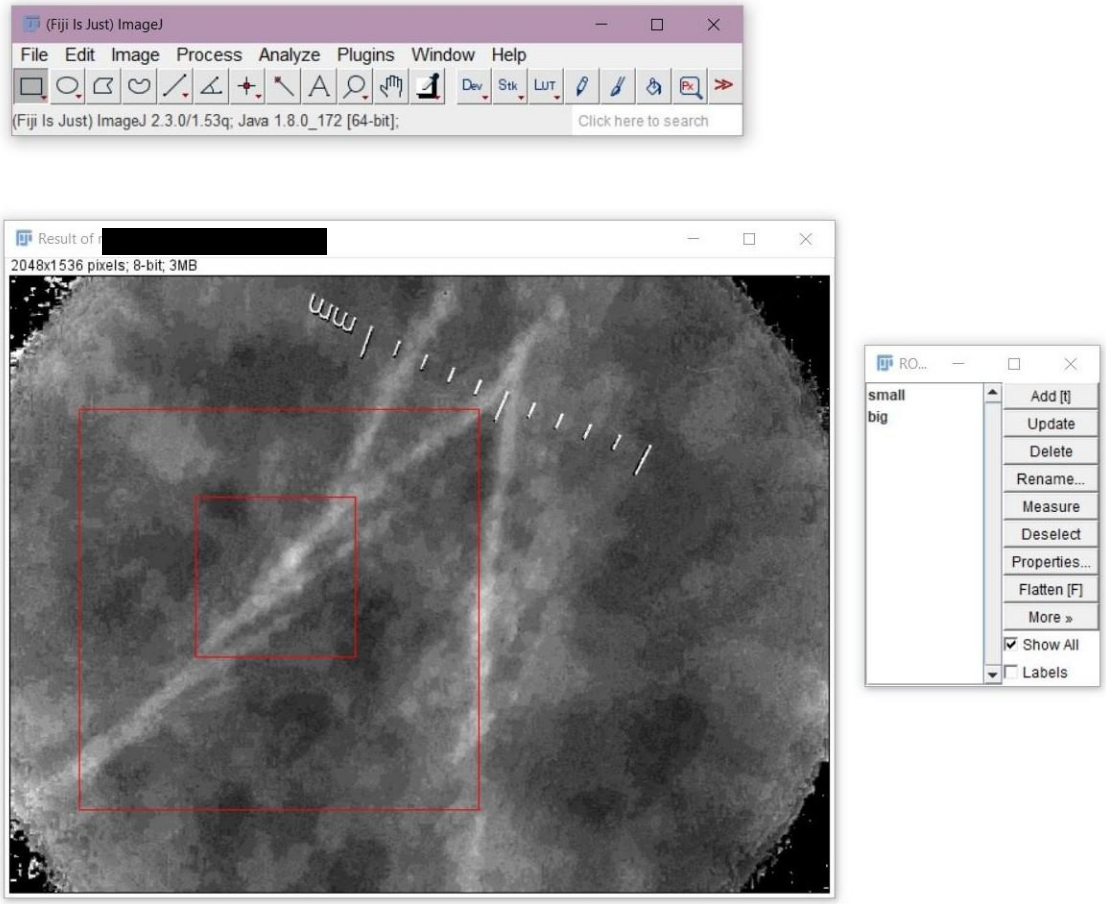

Figure 4.6 Selection of two ROIs

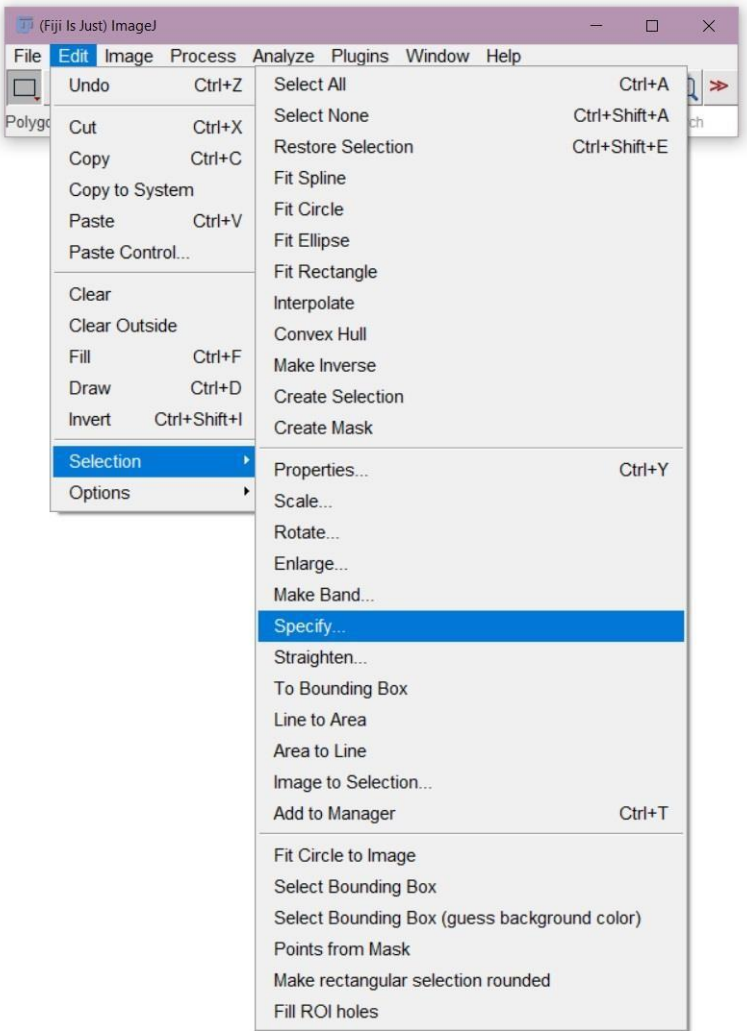

Figure 4.7 Specify command

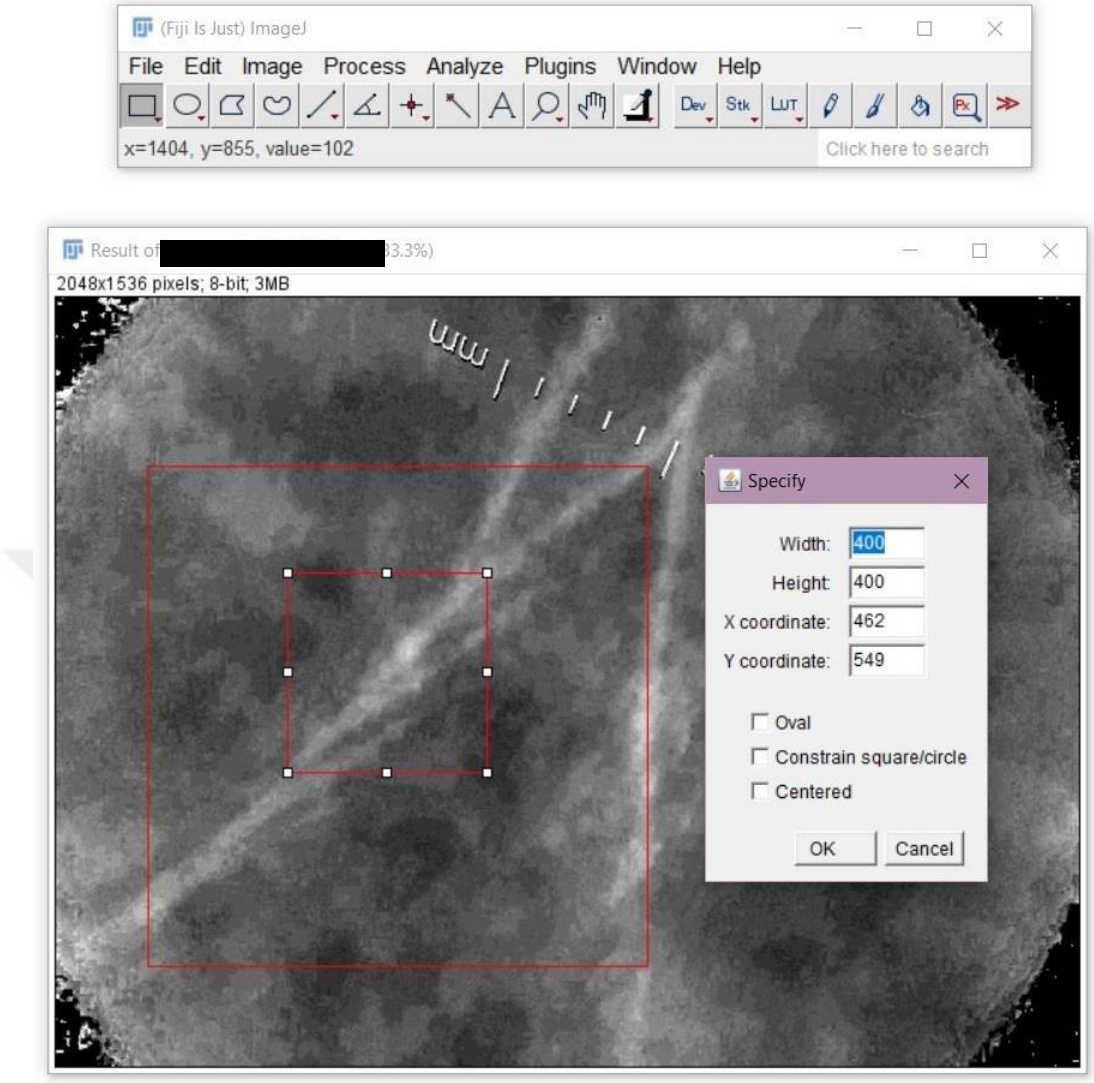

Figure 4.8 The adjustment of dimensions of small ROI

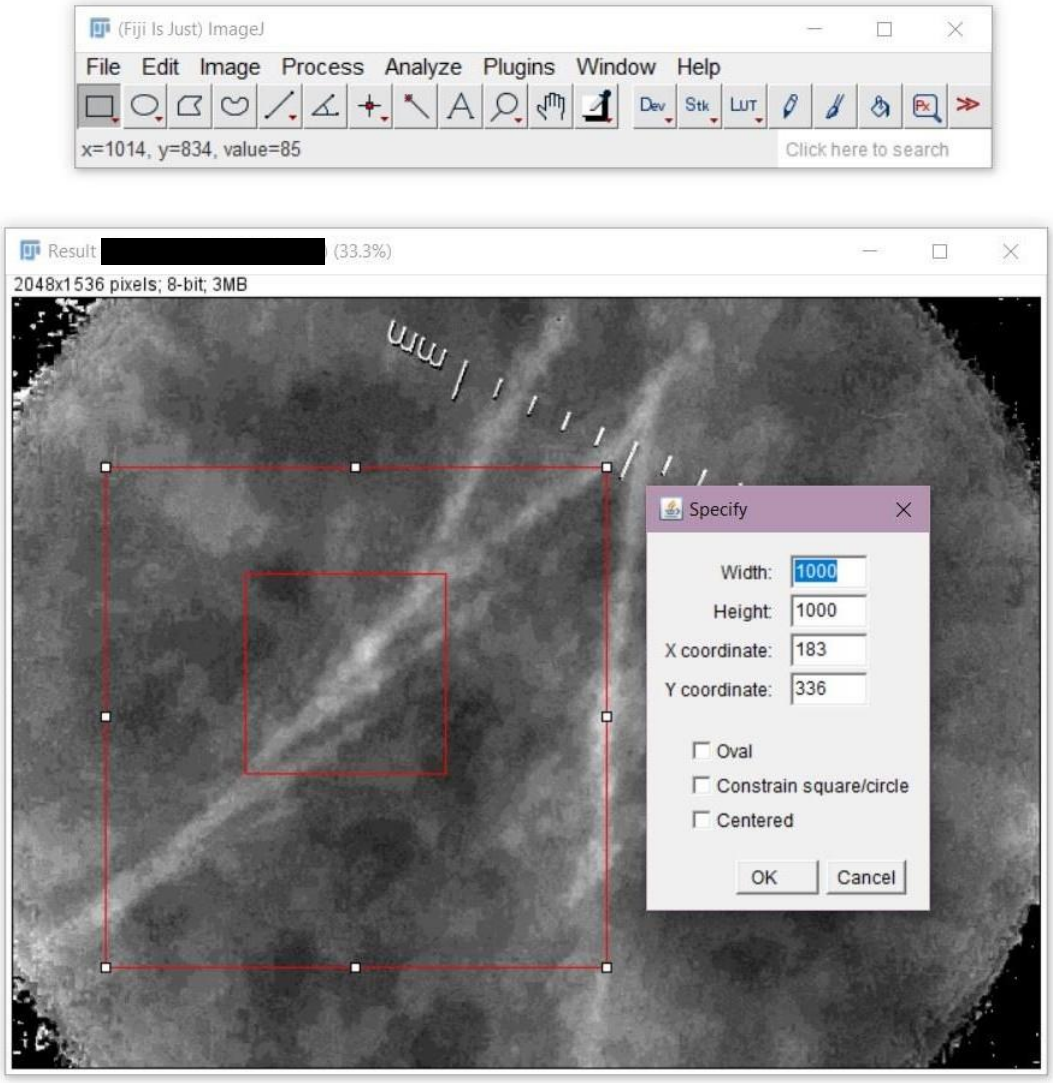

Figure 4.9 The adjustment of dimensions of big ROI

4.3 Finding the Erythema Index value using Image J

Color characteristics of an image is the result of relative shades of red, green, and blue for each pixel. Therefore, average RGB pixel intensity data from ROIs led to estimate the level of Hgb. As described in Chapter 3, the red, green, and blue (RGB) pixels were separated for each image using the Image -> Color -> Split Channels command. Thus, the final image that is obtained from the analyzing process is the difference between the Log Red and Log Green images are gray-scale images. Therefore, it is hypothesized that the gray value of each pixel within the region of

interest has the same correlation with color intensity and thus with erythema index value.

In Figure 4:11, the final image that is obtained at the end of the pre-processing step is demonstrated with different ROIs that are placed inside the image. Figure 4:12, shows Analyze -> Histogram command which displays the histogram of the distribution of gray values in the selected ROI and Figure 4:13, shows Analyze -> Plot Profile command that displays the two-dimensional graph of the intensities of pixels of the selected ROI.

Every selected ROI has its own histogram and graph. Figure 4:14 and Figure 4:15 respectively show big and small ROIs histograms and plot profiles where Figure 4:16 shows the histogram of line ROI.

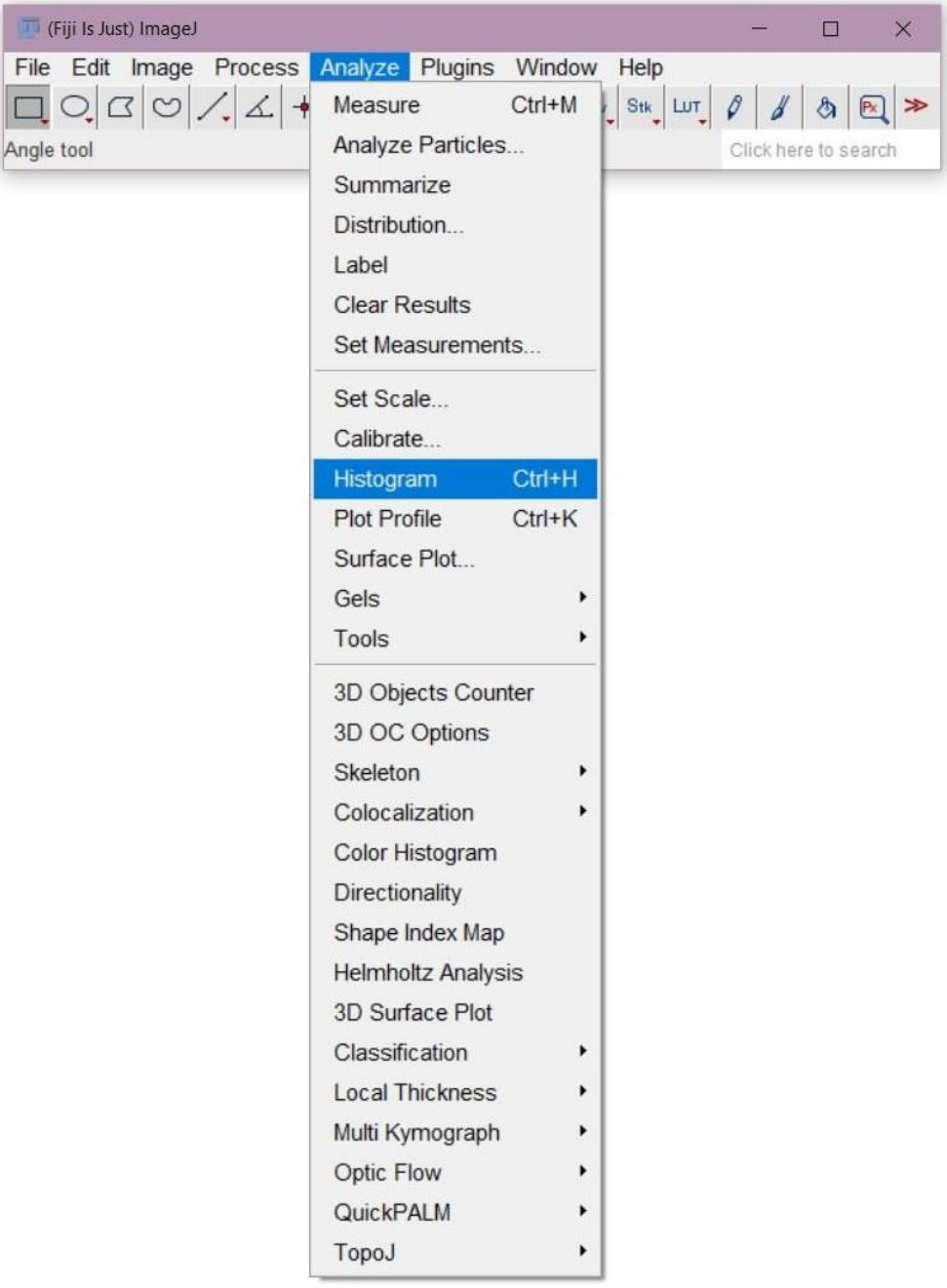

Figure 4.10 Histogram command

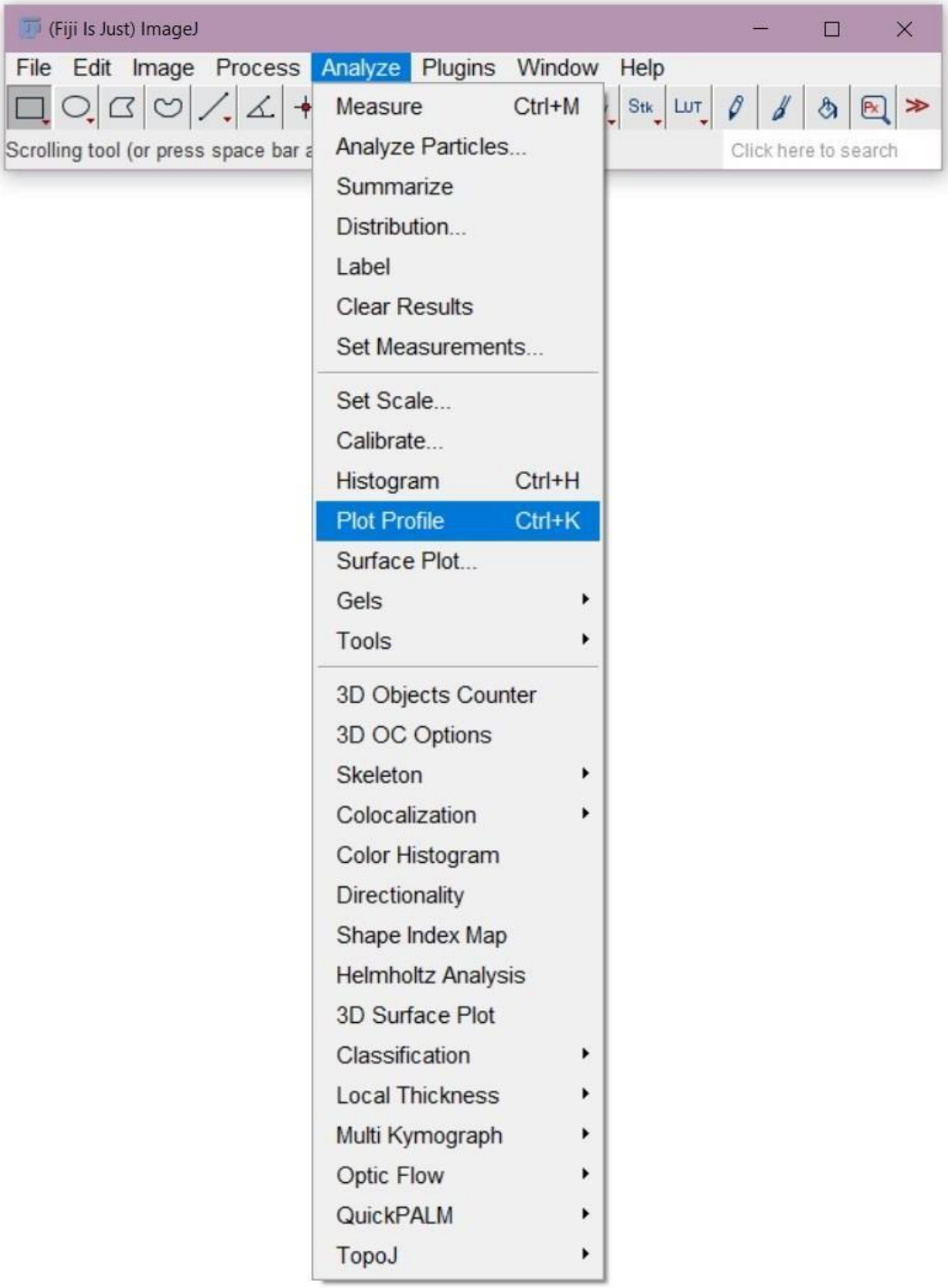

Figure 4.11 Plot profile command

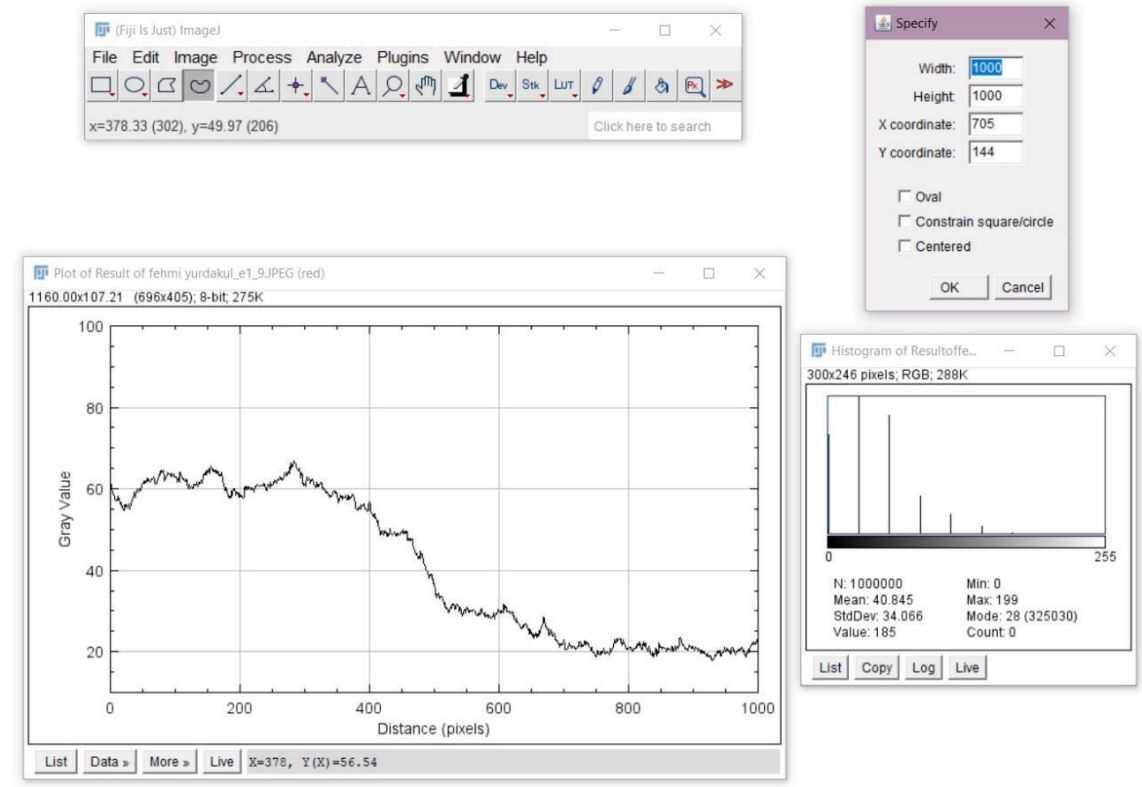

Figure 4.12 Plot profile of Big ROI

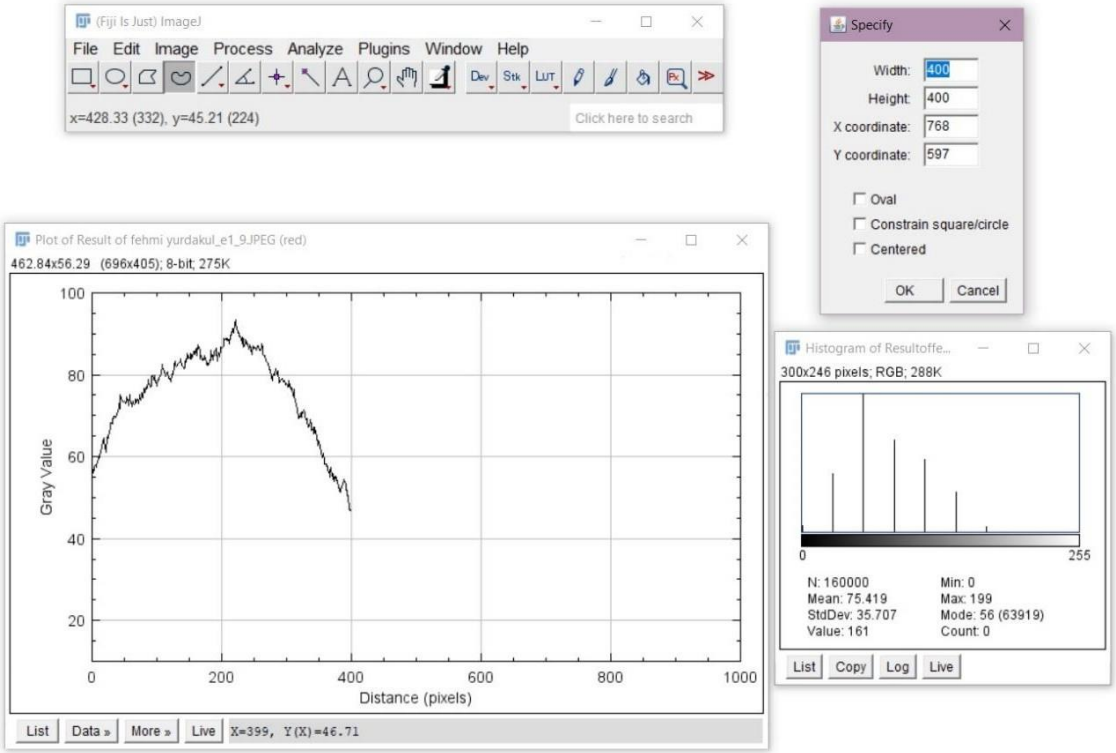

Figure 4.13 Plot profile of Small ROI

Chapter 5: **METHODOLGY**

5.1 Study Design

This study was designed to be conducted in two phases prior to the COVID-19 pandemic. First phase is planned to be the collection of data which includes taking high-resolution images via smartphone attachments and obtaining complete blood count (CBC) results of the experimental groups. And, the second phase is planned as a data analysis phase including the design, development of image processing and deep learning algorithms. However, during the course of this study, the severe acute respiratory syndrome coronavirus 2 (SARS-CoV-2) that causes the new coronavirus illness (COVID-19) appeared and was later identified in the beginning of 2020. [72] All research activities unrelated to COVID-19 including ours, were suspended as a direct result of the lockdown procedures and the closure of the university research centers including Koc University. The study had to be delayed because of this circumstance. Consequently, the study was conducted in four phases.

In the first phase, a limited number of subjects could be recruited to the study due to hospital restrictions. Digital colored images of the palm and finger areas were taken via smartphone camera attachment from subjects. After the covid-19 restrictions started again, the lockdown measures forced us to stay at home and enrolment into new studies also suspended. During this second phase, images of the small study group that were conducted in Koc University Hospital were analyzed and the image processing method was developed.

All procedures were reviewed and approved by the Institutional Review Board (IRB), Koc University (#2019. 189.IRB2.051, named “Anemi Ayırıcı Tanısında ve Takibinde Derin Öğrenme ve Görüntü İşlemeye Dayalı Taşınabilir Non-invaziv Yönteminin Geliştirilmesi”).

In the third phase after the restrictions were eased, more subjects were able to recruit in the study and in the final phase all collected data from phase one and phase third were analyzed.

5.2 Collection of the Data

A feasibility study was conducted for a group of patients who were admitted to Koc University Hospital, Hematology clinics and Lokman Hekim University Hematology and Internal Diseases clinics with the symptoms of anemia and also for the control group. Both subjects who entered the inpatient and outpatient hospitalization, and healthy subjects who scheduled to have their complete blood count (CBC) parameters measured with hematology blood analyzers as part of their clinical care were recruited to this study (n=201). Blood samples were taken using a venous blood draw, which is the hospital's usual procedure, and then their CBC parameter levels were examined using a clinical hematology analyzer. Prior to participating in this study, verbal and written consent were obtained from subjects in accordance with the Koc University Institutional Review Board (IRB) (#2019. 189.IRB2.05) and the Lokman Hekim University regulations.

Subjects whose condition requires inpatient hospitalization mostly already underwent blood sample collection. In this case the copy of their analyzed CBC results within 7 days were collected and the high-resolution images were taken of those patients' palm and finger areas via smartphone camera. Otherwise, their images were taken after the patients' blood samples were collected for the CBC analysis.
The images of anemia in- and outpatients were taken with an Apple iPhone 7 (Apple Inc., California, USA) using the image settings at its defaults. All images also were taken at a fixed distance and with the same illumination via smartphone dermatoscope attachments for the patients' palm and finger region.

The dermoscopic examinations in the palm area were performed with a polarized / non-polarized-light handheld dermatoscope (DermLite DL4; 3Gen, San Juan Capistrano, CA, USA) and also iPhone 7 connection kits.
To prevent data loss in the high-resolution quality, images were not transferred through e-mail or message platform programs in the mobile phone, instead they were transferred from the smartphone used in this study to the rented iCloud (Apple Inc., California, USA) platform and then a computer to be analyzed.

In order to insert a dermatoscope in the crease region and obtain high quality photos without causing blurring, subjects were encouraged to expand their crease area rather than open their hands excessively, which might cause alterations in blood flow.

As the attached dermatoscope has its own non-standardized ambient lighting, image qualities were not influenced by variable light conditions that affect the diagnosis outcomes. The glass plate of the dermatoscope lens was placed on the area of the patient's fingers and palm.

CBC parameters of patients' other than Hgb including hematocrit (HCT), red blood cell count (RBC), mean cell volume (MCV) and red blood cell distribution width (RDW) are also analyzed and conducted via same clinical hematology analyzer (Sysmex, Sysmex Corporation, Kobe, Japan).

5.3 Determination of a body region of interest

As it has been mentioned in the Introduction chapter, physical examination of pallor in conjunctiva, palmar creases, fingers and nail beds is used in diagnosis of anemia due to their lack of containing melanocytes. Therefore, in these regions, the production of melanin is suppressed and Hgb is the main factor influencing the skin tone. [57] Whereas fluctuation of Hgb levels cause the changing in skin tone. Many studies have focused on this assumption to evaluate the alterations in skin tone to estimating Hgb levels, like discussed in the literature review.

The study's original aim was to examine the interior of the hand, including the fingers and palm. Therefore, both palm and fingers were designated as the area to focus on, and images were taken accordingly.

Figure 5:1 shows the colored image of the subject's finger and Figure 5:2 shows colored image of the same subject's palm region. Both images were used for image analysis.

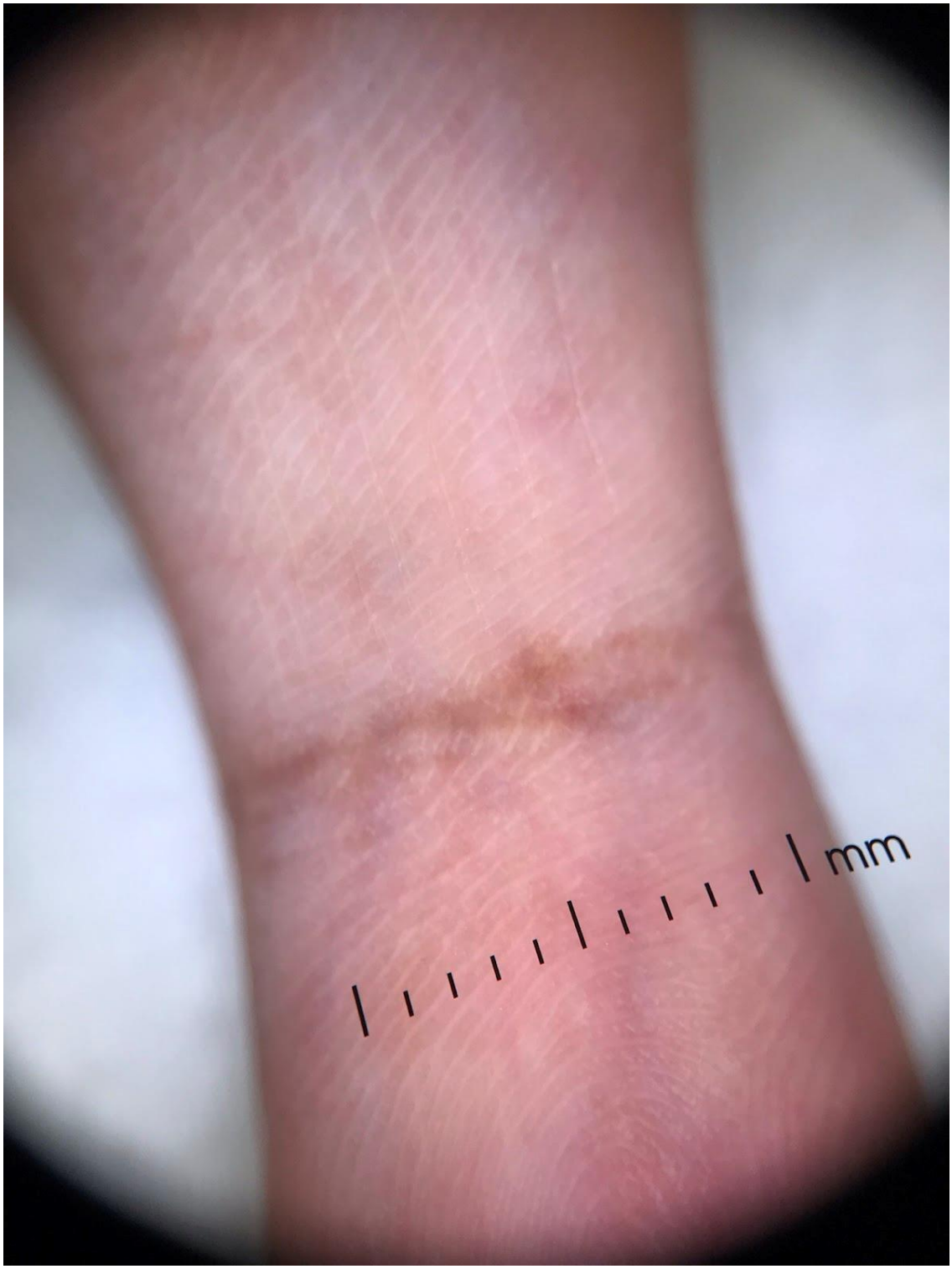

Figure 5.1 Colored image of the subject's finger

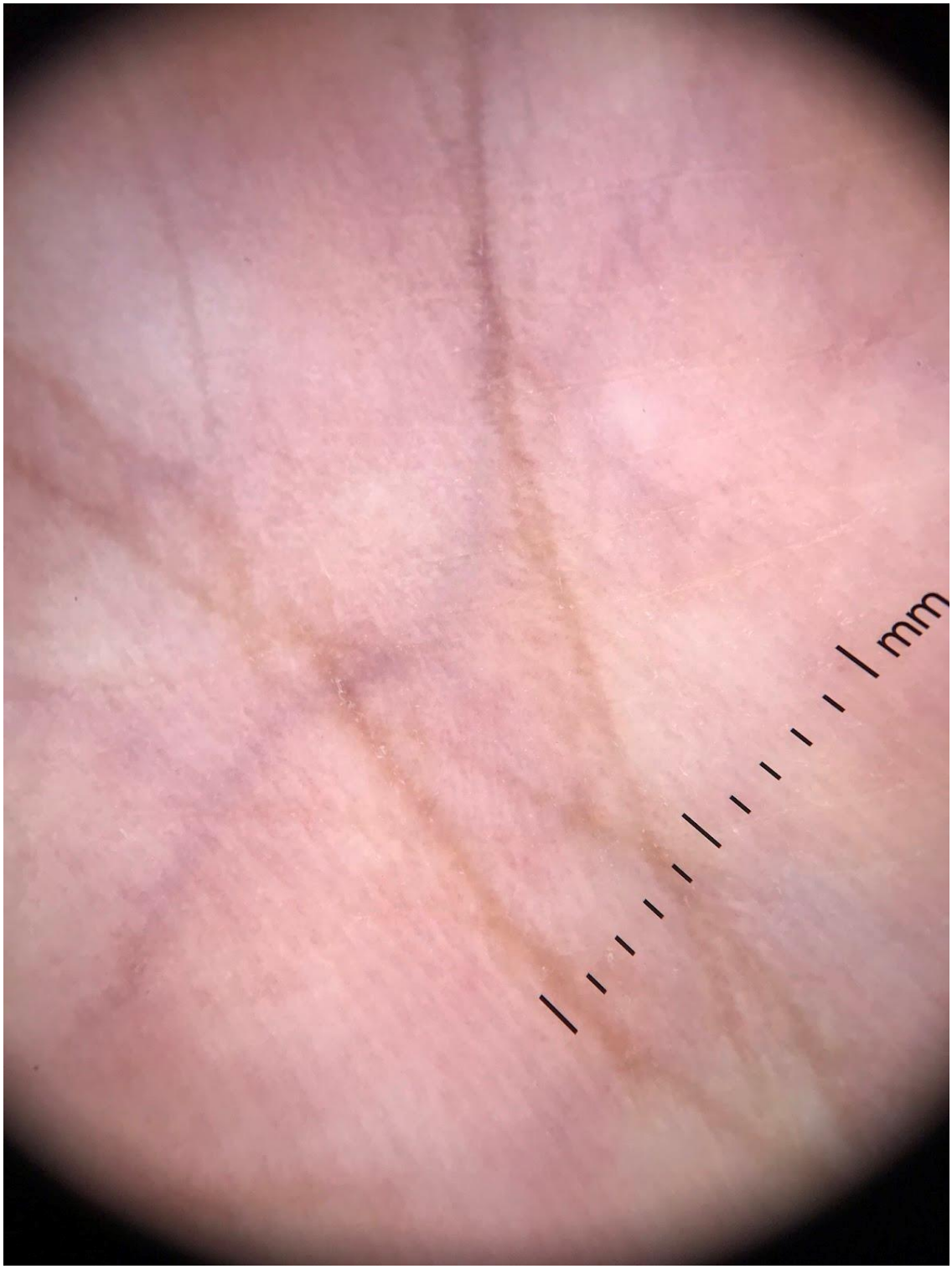

Figure 5.2 Colored image of the same subject's palm region

High resolution images were taken with the macro-lens as smartphone-based skin screening attachment that made it possible to capture images of palm and finger regions (DermLite DL4; 3Gen, San Juan Capistrano, CA, USA) very close up, allowing us to see tiny details.

In Figure 5:3 the hand image that was taken from distance demonstrates the different regions that were aimed to analyze for the determination of the body region of interest. However, during the course of phase one, the limitation of the finger crease area as an image site was addressed. In addition, our analysis in the phase two proved that there were no correlations between the erythema index value of finger crease images and the CBC hemoglobin levels.

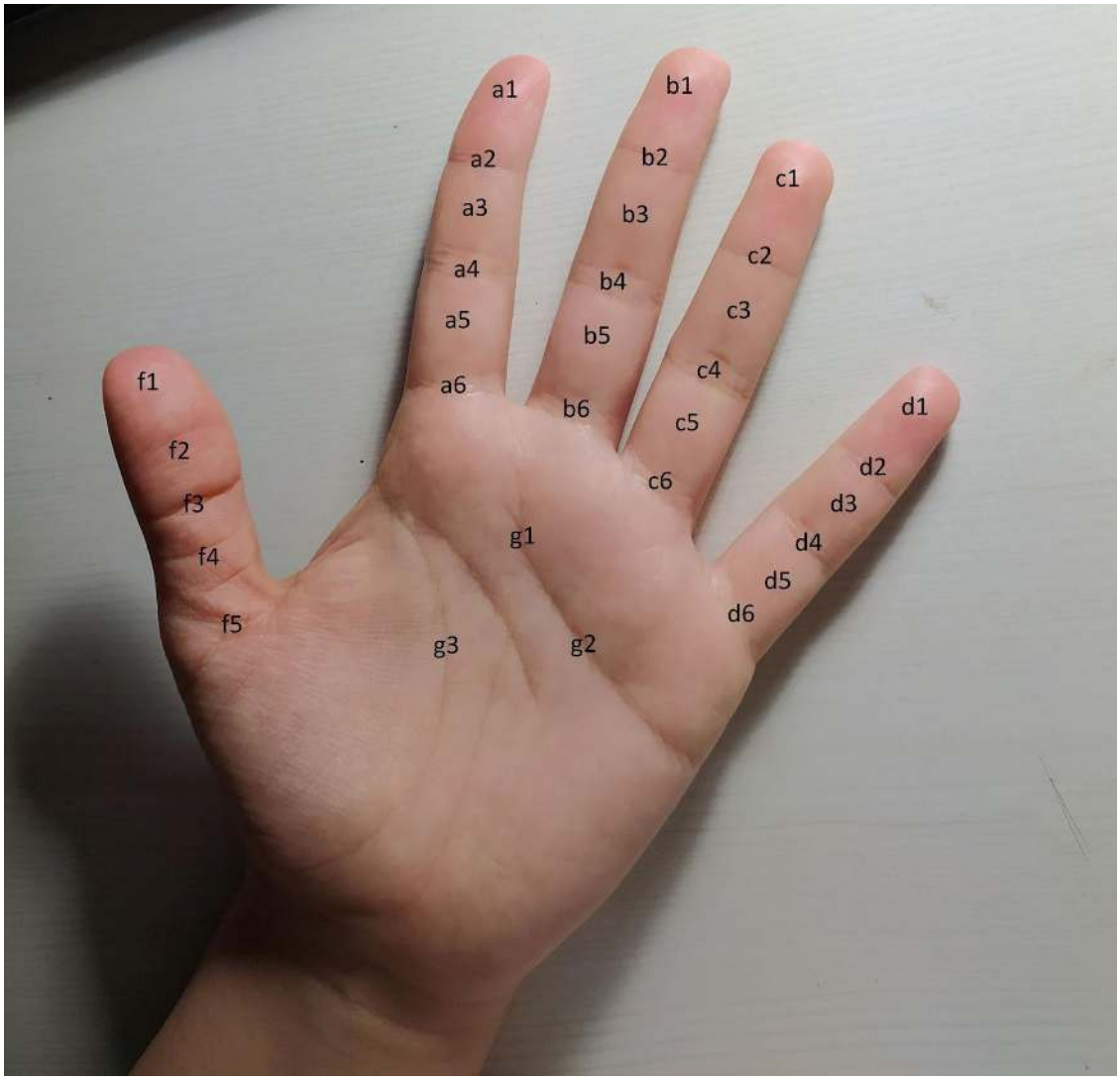

Figure 5.3 Determination of the body region of interest

5.4 Using Smartphone Attachment

In this study, smartphone-based skin screening attachment (Figure 5:4) was used (DermLite DL4; 3Gen, San Juan Capistrano, CA, USA) to obtain high resolution images with the macro-lens. As the attached dermatoscope has its own non-standardized ambient lighting, photos are prevented from being affected by external light sources. Skin screening attachment also ensures consistent background lighting conditions. In order to see details from the epidermis and top layers of the dermis, surface reflections can be removed with the dermatoscope. With the help of connection kits, (Figure 5:5) a dermatoscope was attached to the smartphone (Figure 5:6). The quality of images was standardized with help of the handle that minimizes the error of the user.

Figure 5.4 Smartphone-based skin screening attachment

Figure 5.5 Connection Kits

Figure 5.6 Smartphone with dermatoscope attachment

Chapter 6: **EXPERIMENTAL SETUP**

This study was originally planned to be carried out only at Koc University Hospital, Koc University School of Medicine, Istanbul, Turkey. However, during the course of this study, the COVID-19 pandemic has emerged. [77] All research activities unrelated to COVID-19 including ours, were suspended as a direct result of the lockdown procedures and the closure of the university research centers including Koc University. Due to the risk of spreading COVID-19, hospital admissions were prohibited. This situation caused the study to be postponed for a while. Even after the partial lifting of restrictions, It was particularly challenging to recruit participants for the study. After being able to enter the hospital, in the first 6 months of the clinical assessment phase of this study, patients who were admitted to Koc University Hospital, Hematology clinic were recruited to participate in this project. However, due to the emergence of the Covid-19 pandemic, hospitals had restricted the number of patients admitted and the intended number of patients was not reached in the stipulated time when the study was planned. While the pandemic restrictions were still going on, certain hospitals were approached to find out which hospital had the largest patient volume in order to reach the required number of patients. After obtaining the necessary authorizations from both Koc University School of Medicine and Lokman Hekim University School of Medicine, the study was continued at Lokman Hekim University Hospital, Lokman Hekim University School of Medicine, Ankara, Turkey to expand the patient population.

The experimental setup (Figure 6:1) consists of a dermatoscope (DermLite DL4; 3Gen, San Juan Capistrano, CA, USA), connection kit (3Gen, San Juan Capistrano, CA, USA) and smartphone (Apple iPhone; Apple Inc., California, USA). Connection kit works as a phone case and is easily put on the phone. With the built-in magnet, the connection kit attaches to the dermatoscope. This setup allows taking images from the palm. (Figure 6:2) and enables microscopic visualization of the palmar crease. (Figure 6:3)

Figure 6.1 Experimental Setup

Figure 6.2 Illustration of experimental setup

Figure 6.3 Illustration of a microscopic visualization of the palmar crease

6.1 *Image Analysis*

As it was mentioned in the Chapter 5, images were transferred from the smartphone used in this study to the cloud platform which is iCloud (Apple Inc., California, USA) and then to a computer to be analyzed in order to prevent data loss in the high-resolution quality. (Figure 6:4)

All images were 32-bit, RGB images with JPEG (Joint Photographic Experts Group) format. First assessment was manually evaluating images to ensure data validation. In this process, the quality of every image was evaluated manually by different experimentalists to eliminate observational error. Additionally, all 201 patients had their palmar crease color evaluated by a doctor who was unaware of their Hgb levels from their images. Images of each study participant were sequentially evaluated by an observer who was unaware of the diagnosis, physical findings, and laboratory results. The qualification list mainly contained the amount of blur in the images, light reflection, discoloration of fingers and palms, focusing errors and subjects' specifications like loss of a hand or progressive loss of motor control. Total 113

participants were excluded from the study due to not being able to satisfy the necessities from the qualification list.

Images were analyzed with ImageJ free software (Rasband, W.S., ImageJ, U. S. National Institutes of Health, Bethesda, Maryland, USA). Figure 6:4 illustrates the image transfer from smartphone to ImageJ software. Images were split into red, green, and blue components. Logarithm functions were applied to the red and green images to transform them into logarithmic red and green images. Logarithmic green images were subtracted from the logarithmic red images to obtain the difference between logarithmic red and green images. After image processing methods based on brightness and contrast adjustment and RGB color pattern were applied to images to calculate the EI parameter for the palm and finger areas, the region of interests (ROIs) from every selected image were manually chosen. The pixels inside the selected region of interest were used for analysis. Each operation was performed multiple times as the original images were split. Every mean value of each image was recorded. By comparing the results to known hemoglobin values and repeating the calculation after modifying the constants, an iterative method was used to develop the formula using the pixel values from the images and standard and constant values. The obtained formula then applied to every measured mean value. The estimated erythema index value was then compared to CBC measured hemoglobin results.

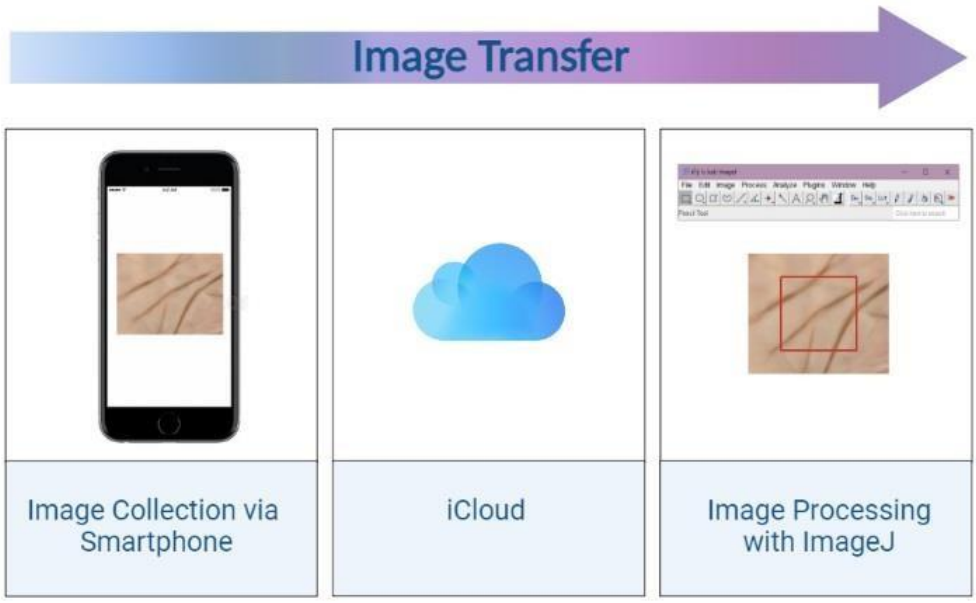

Figure 6.4 Schematic description of the image transfer

Chapter 7: **RESULTS AND DISCUSSION**

7.1 Distribution of Study Population

7.1.1 Distribution of Study Population by Gender and Age

During the course of the project, as shown in Figure 7:1, n=68 subjects participated in this study at Koc University Hospital and n=133 patients participated in this study at Lokman Hekim University Hospital. Which results in a total of n=201 participants. Participants were admitted to both hospitals with the symptoms of anemia and also for the control group. As shown in Figure 7:2, 30 female subjects and 38 male subjects were enrolled in this study at Koc University Hospital, where 96 female subjects and 37 male subjects were enrolled in this study at Lokman Hekim University Hospital. Total of 126 female subjects and 75 male subjects were enrolled in this study. (Figure 7:3)

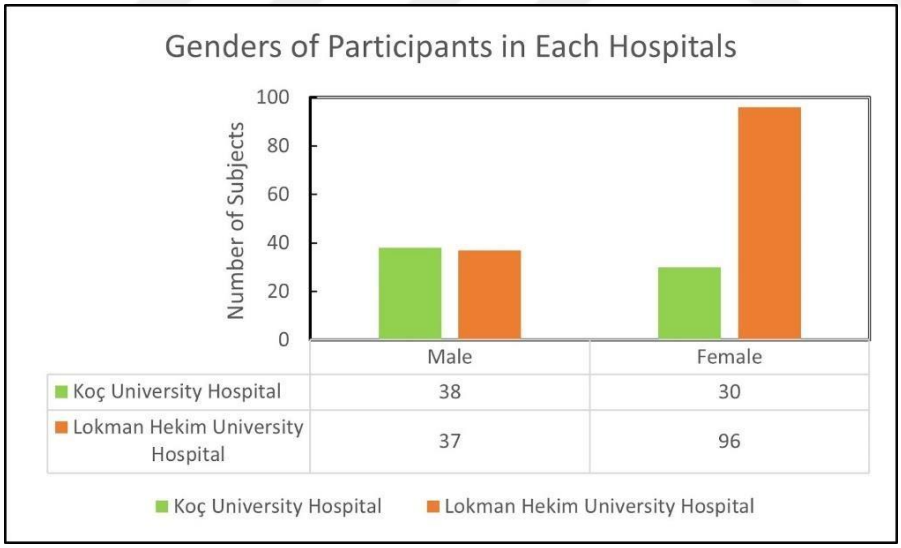

Figure 7.1 Gender of subjects in each hospitals

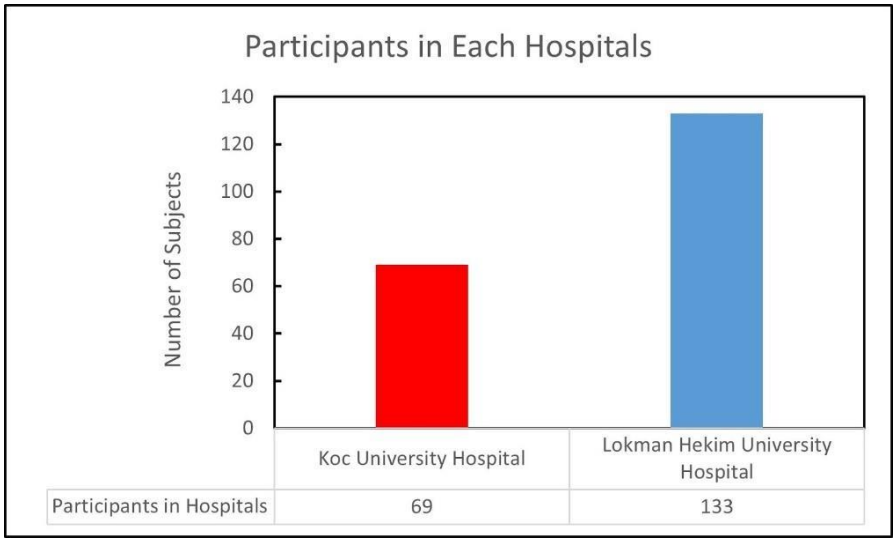

Figure 7.2 Number of subjects in each hospitals

Ages of the subjects ranged from 15 to 93. The study population's ages were divided into groups of 15–29, 30-39, 40–49, 50–59, 60–69, 70–79, and ≥80 years. As shown in Figure 7:4, there are 45 subjects between the ages of 15-29, 21 subjects between the ages of 30-39, 26 subjects between the ages of 40-49, 33 subjects between the ages of 50-59, 38 subjects between the ages of 60-69, 24 subjects between the ages of 70-79, and 14 patients over the age of 80.

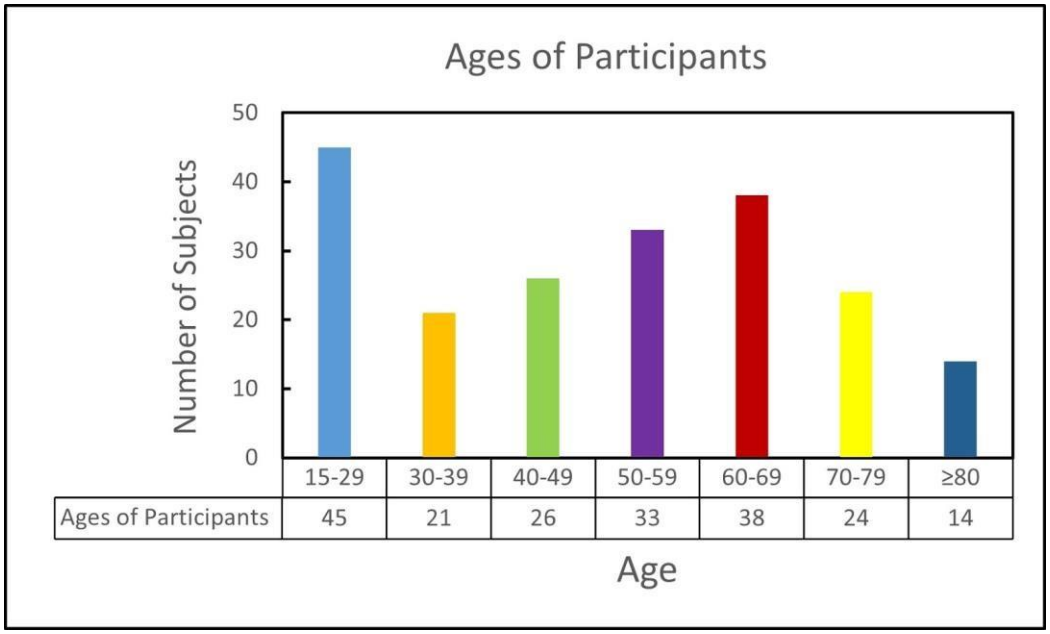

Figure 7.3 Ages of the participants

7.1.2 Distribution of Study Population by Hgb Level

Subjects participating in this study had hemoglobin levels ranging from 6.1 to 18.9. This allowed the inclusion of different HGB values seen in the general population. (Figure 7:4)

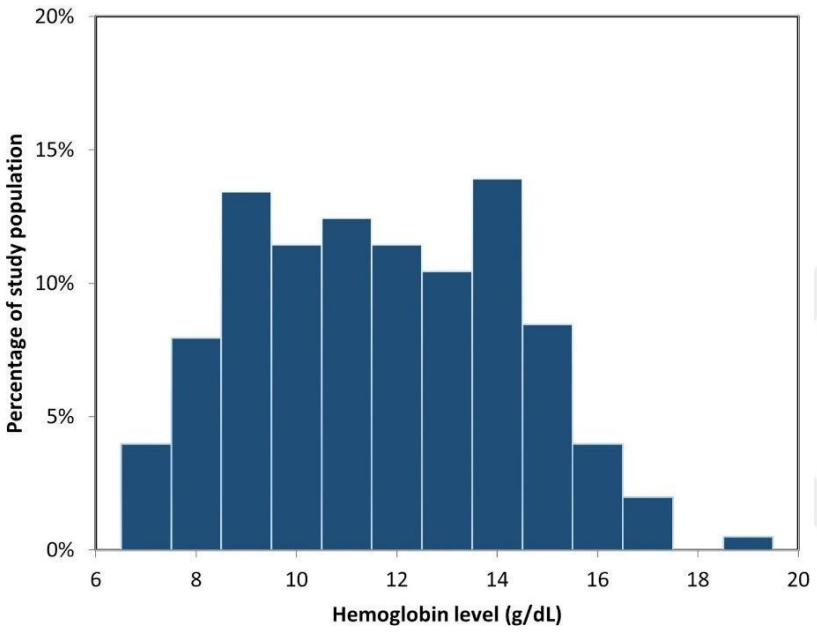

Figure 7.4 Hemoglobin level distribution of study population

As seen in Table 7.1, according to the standards established by the World Health Organization (WHO), anemia is divided into categories of normal, mild, moderate, and severe.

When the hemoglobin values of the subjects are examined with this reference, 11.9% of the subjects were severe, 36.8% of the subjects were moderate, 10.9% of the subjects were mild and 40.3% of the subjects were non-anemic. The pie chart in Figure 7:5 was made to represent these statistics visually.

Table 7.1 Classification of Anemia According to the World Health Organization (WHO) [1]

	Hemoglobin Level (g/dL)			
		Anemia		
Gender	Non-anemia	Mild	Moderate	Severe
Women (non-pregnant and ≥ 15 years old)	≥ 12	11 – 11.9	8 – 10.9	< 8
Men (≥ 15 years old)	≥ 13	11 – 12.9	8 – 10.9	< 8

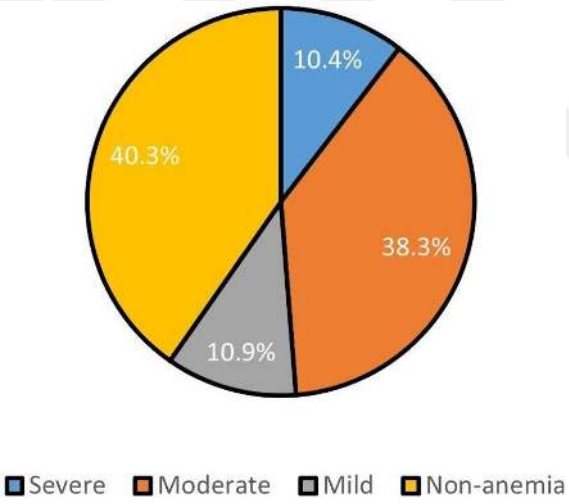

Figure 7.5 Percentage of cases in the study population

7.1.3 Distribution of Study Population by other CBC parameters

Subjects participating in this study had mean corpuscular volume (MCV) levels ranging from 56.4 to 132.8. (Figure 7:6)

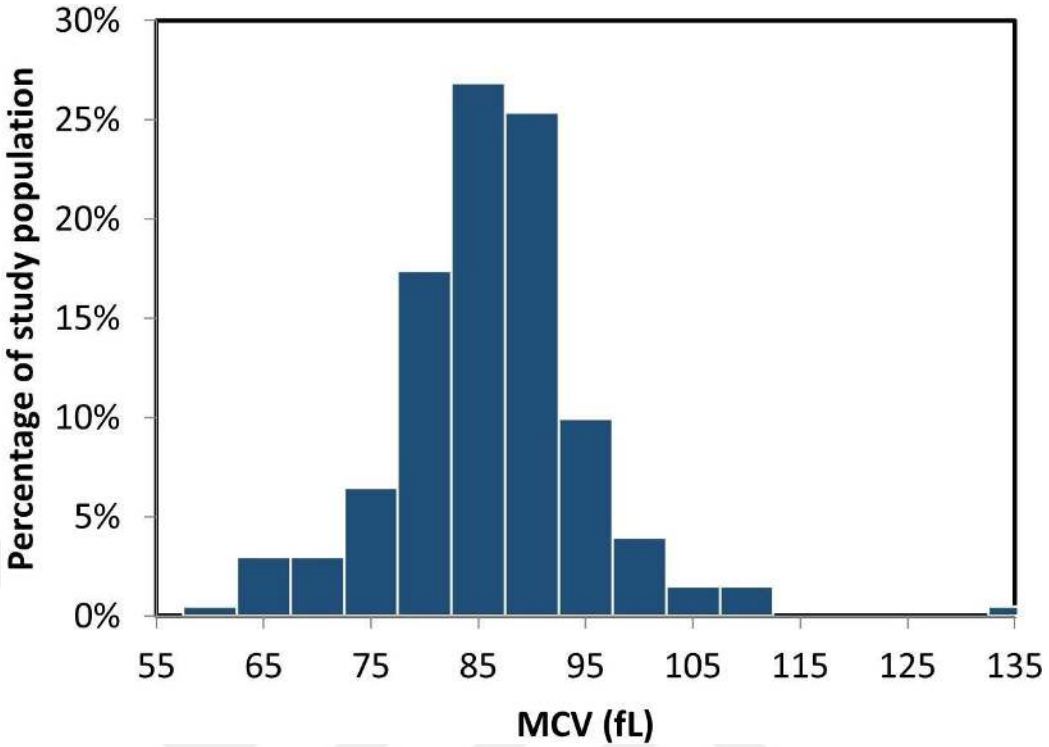

Figure 7.6 MCV level distribution of study population

Subjects participating in this study had red cell distribution width (RDW) levels ranging from 9.5 to 24.7. (Figure 7:7)

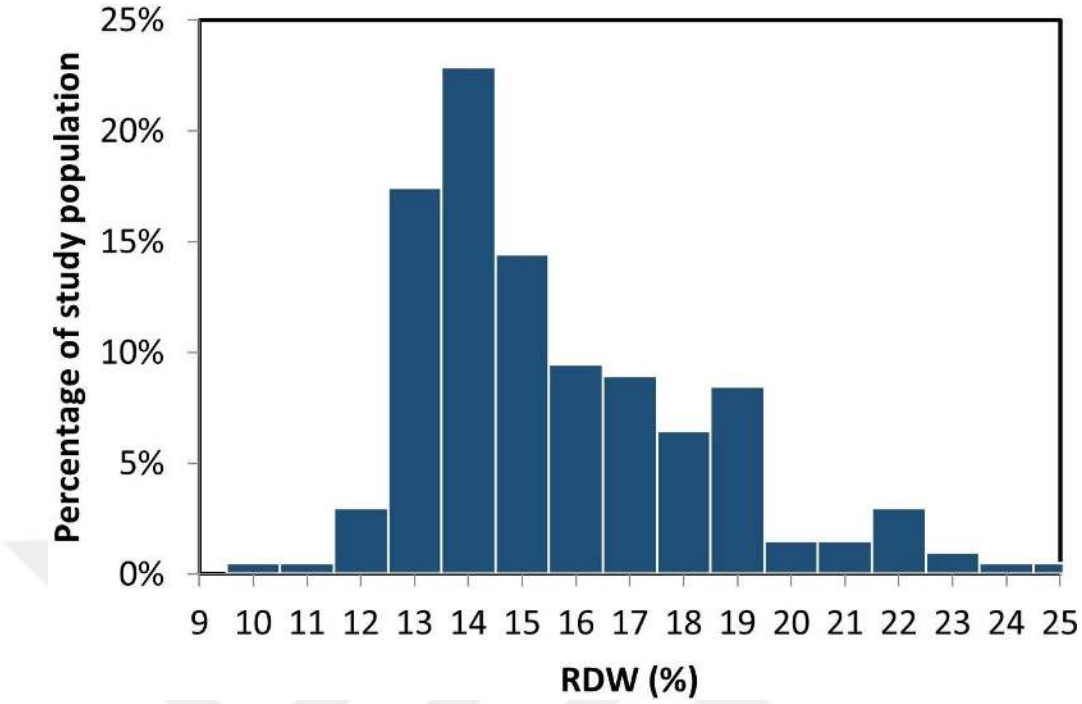

Figure 7.7 RDW level distribution of study population

Subjects participating in this study had hematocrit (HCT) levels ranging from 17 to 54.5. (Figure 7:8)

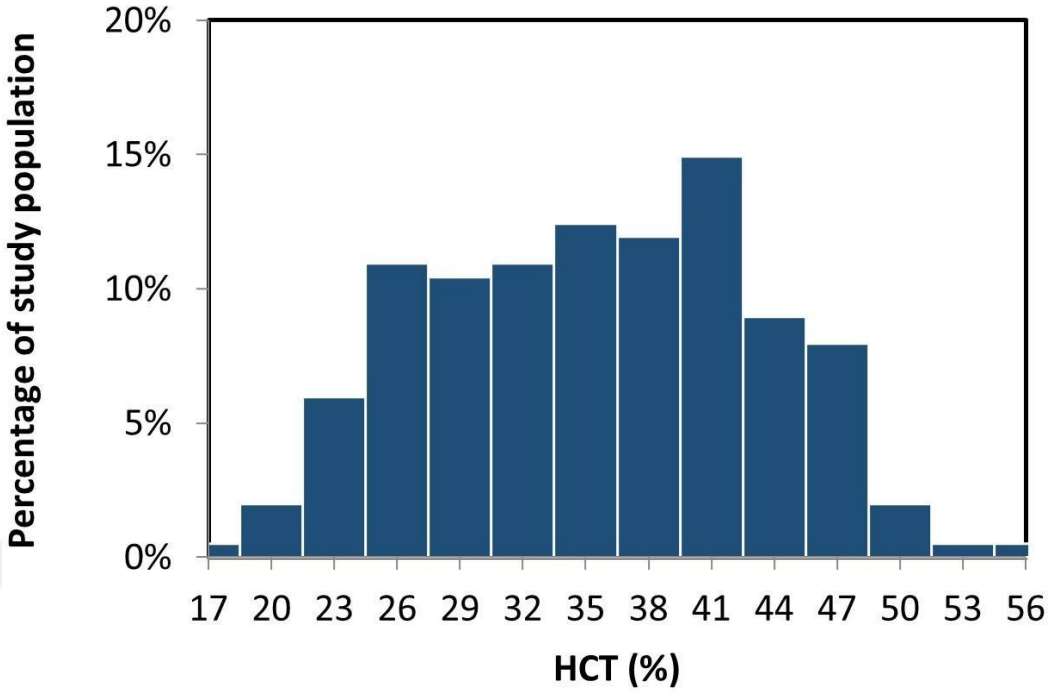

Figure 7.8 HCT level distribution of study population

Subjects participating in this study had red blood cell count (RBC) levels ranging from 1.95 to 9.92. (Figure 7:9)

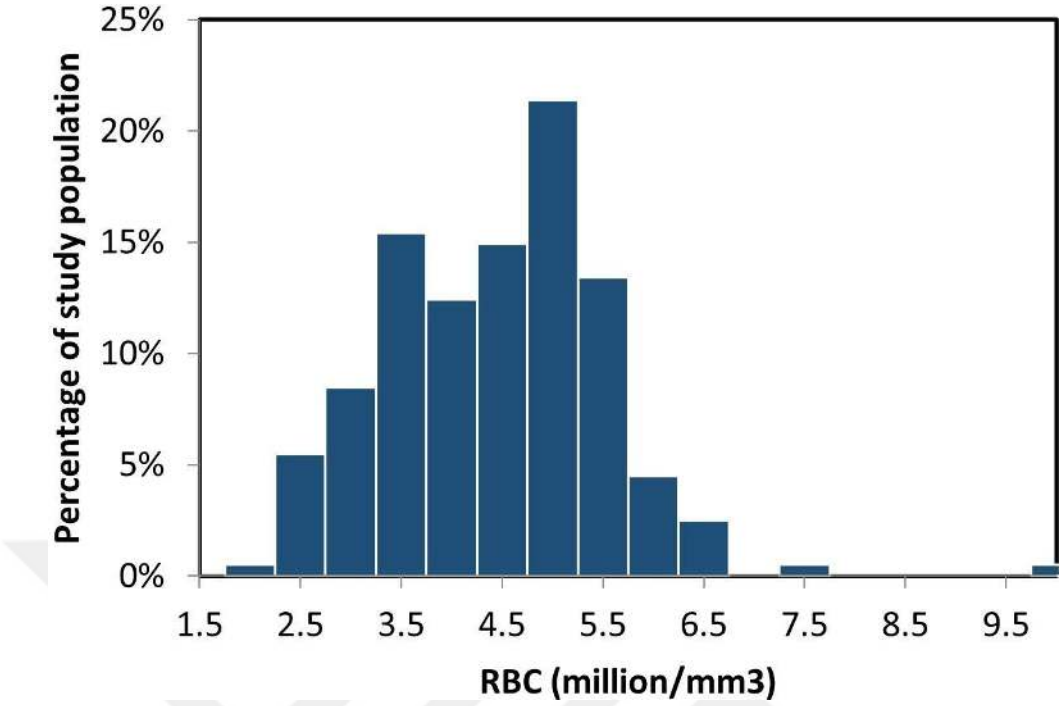

Figure 7.9 RBC level distribution of study population

7.2 Data Selection

7.2.1 Selection of patients to be included in the study

As it mentioned in the Chapter 5, all images that are taken from the subjects were evaluated manually as a pre-processing phase in order to eliminate the subjective and operational errors during data collection. A physician who was uninformed about the patients' Hgb levels assessed the color of the palmar creases in all 201 patients. The study excluded participants with pigmentation problems like vitiligo, albinism, contact dermatitis of the hands, and scarring of the palms. In one case, the patient's one hand was amputated after the images were taken and this subject was excluded from the study. Some pictures were shifted or repositioned as a result of the photographer's error to eliminate this; it was intended to exclude all images with low quality and low resolution. Since all the photos were taken in the hospital during the most restrictive Covid precautions, it was not possible to shoot palm images of the same patient again.

This resulted in excluding the patient if their palm images did not meet the required criteria.

Distribution of Selected Study Population by Hgb Level

Following all the data exclusion process, a total of 89 subjects' palm images and CBC blood Hgb levels were analyzed in this study and selected subjects also had hemoglobin levels ranging from 7.1 to 18.9. (Figure 7:10)

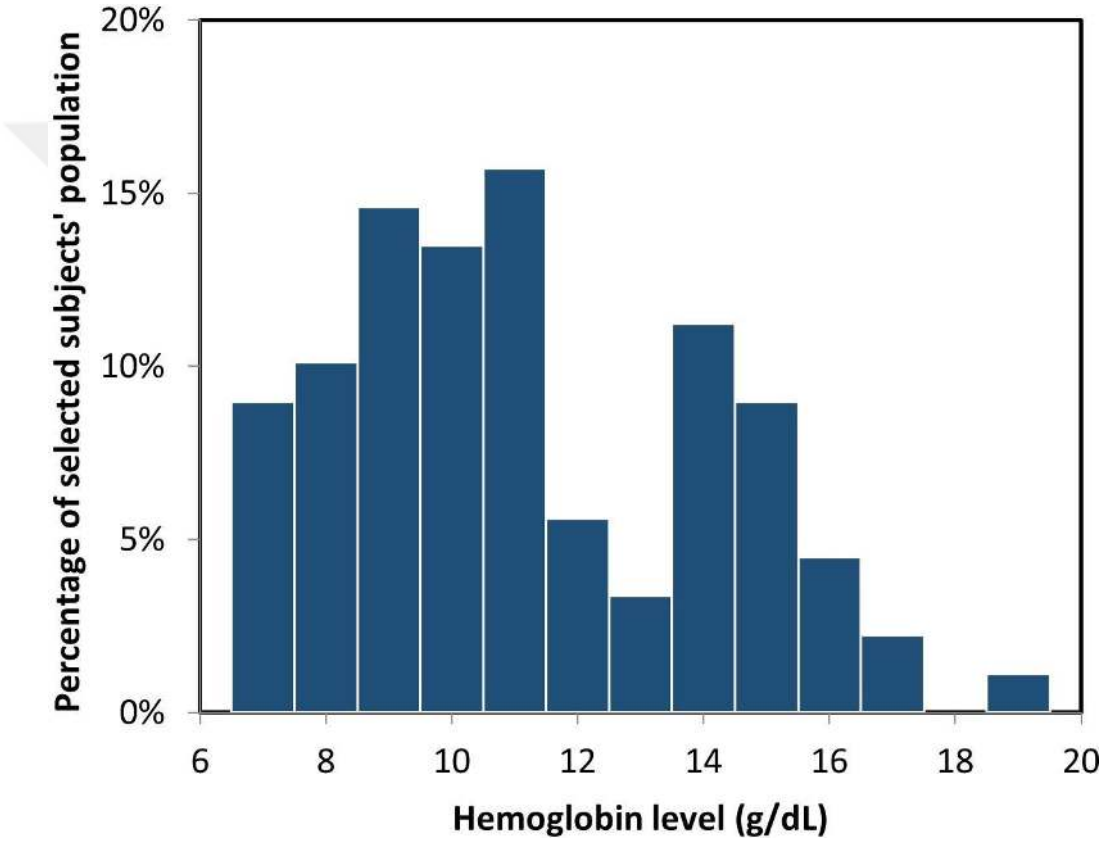

Figure 7.10 Hemoglobin level distribution of selected subjects' population

Selected subjects participating in this study had also hematocrit (HCT) levels ranging from 17 to 54.5. (Figure 7:11)

Distribution of Selected Study Population by other CBC parameters

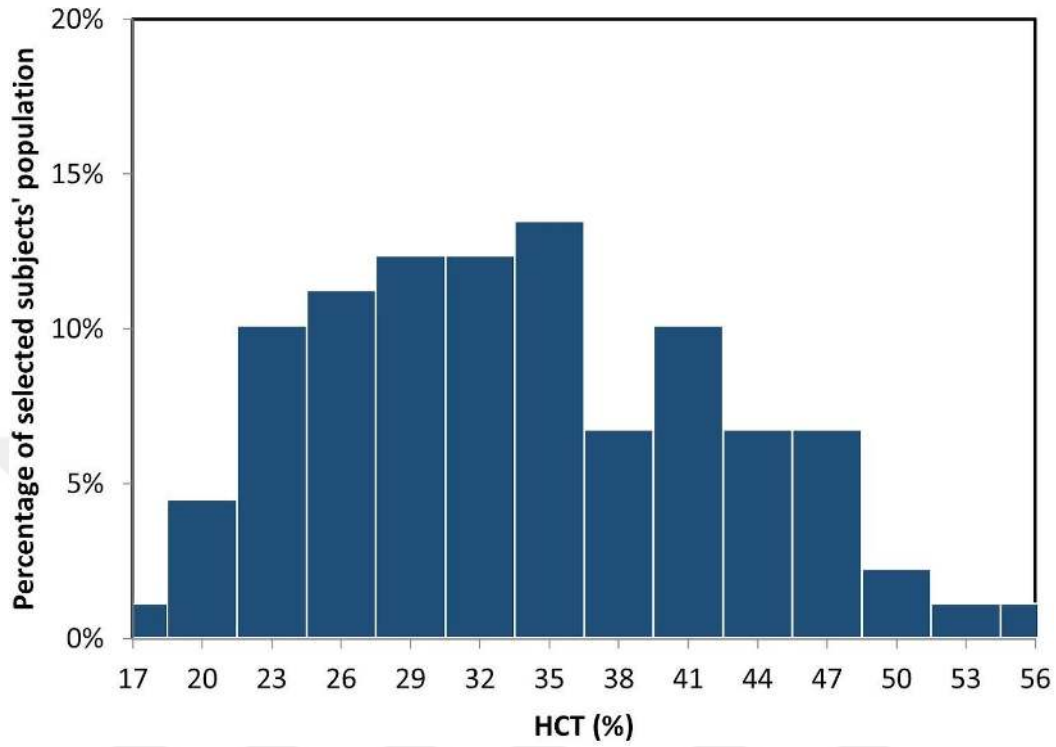

Figure 7.11 HCT level distribution of selected subjects' population

Selected subjects participating in this study had mean corpuscular volume (MCV) levels ranging from 60.2 to 105.2. (Figure 7:12)

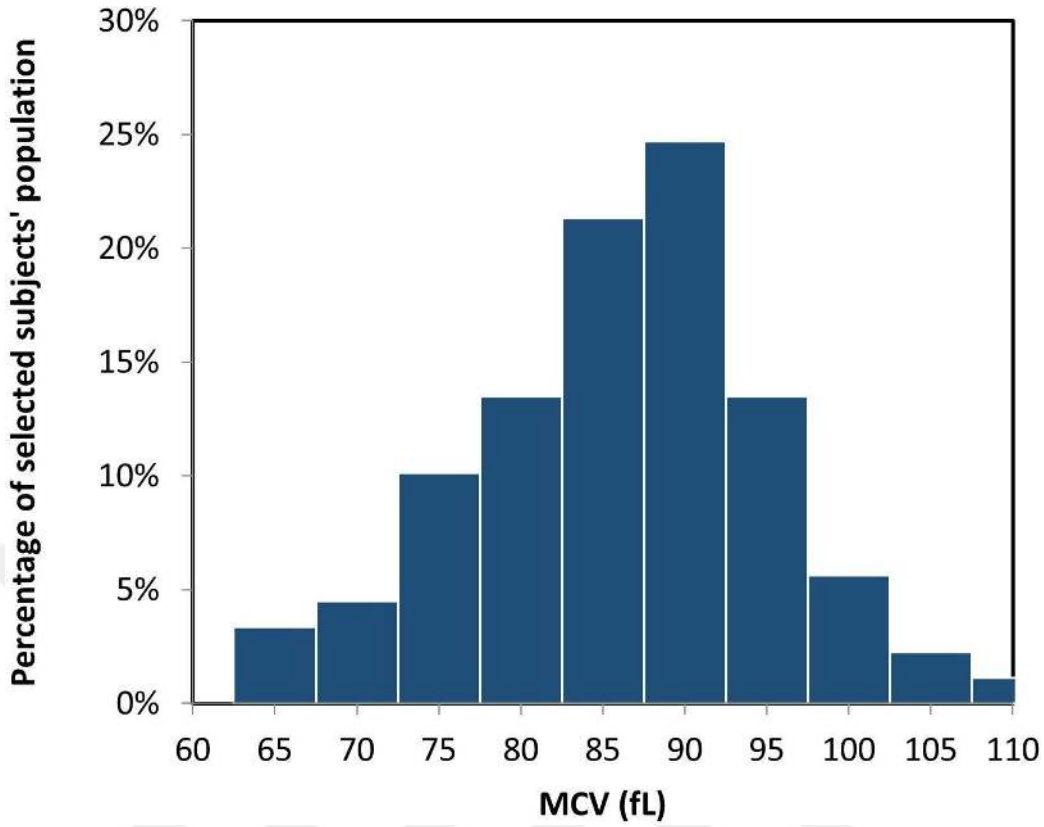

Figure 7.12 MCV level distribution of selected subjects' population

Selected subjects participating in this study had red cell distribution width (RDW) levels ranging from 9.5 to 23.2. (Figure 7:13)

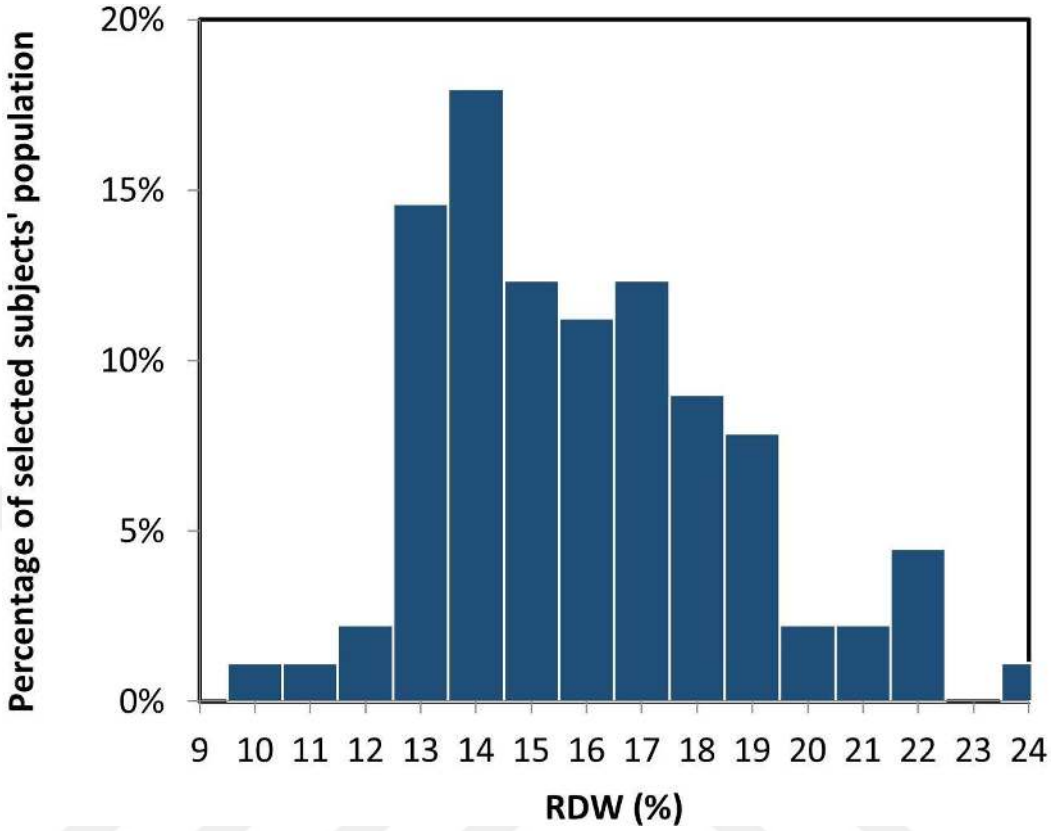

Figure 7.13 RDW level distribution of selected subjects' population

Selected subjects participating in this study had red blood cell count (RBC) levels ranging from 2.03 to 9.92. (Figure 7:14)

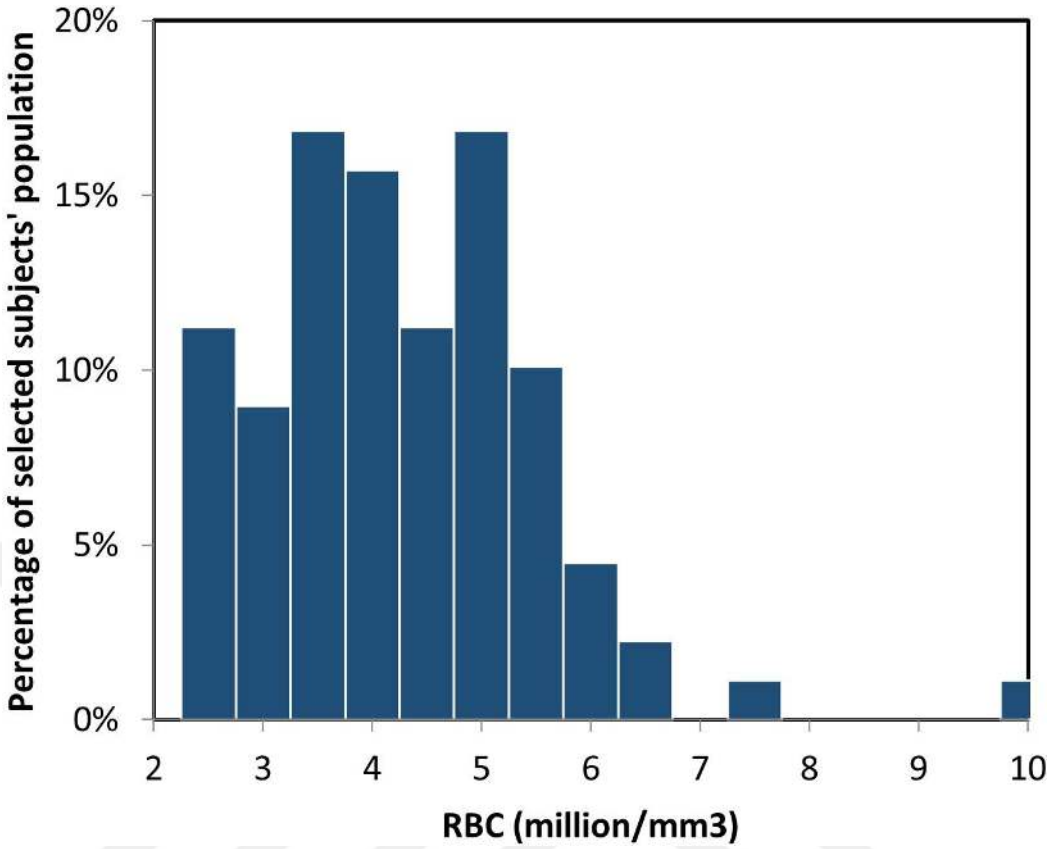

Figure 7.14 RBC level distribution of selected subjects' population

When the hemoglobin values of the subjects are examined with the reference from Table x, 16.9% of the subjects were severe, 44.9% of the subjects were moderate, 7.9% of the subjects were mild and 30.3% of the subjects were non-anemic. The pie chart in Figure 7:15 was made to represent these statistics visually.

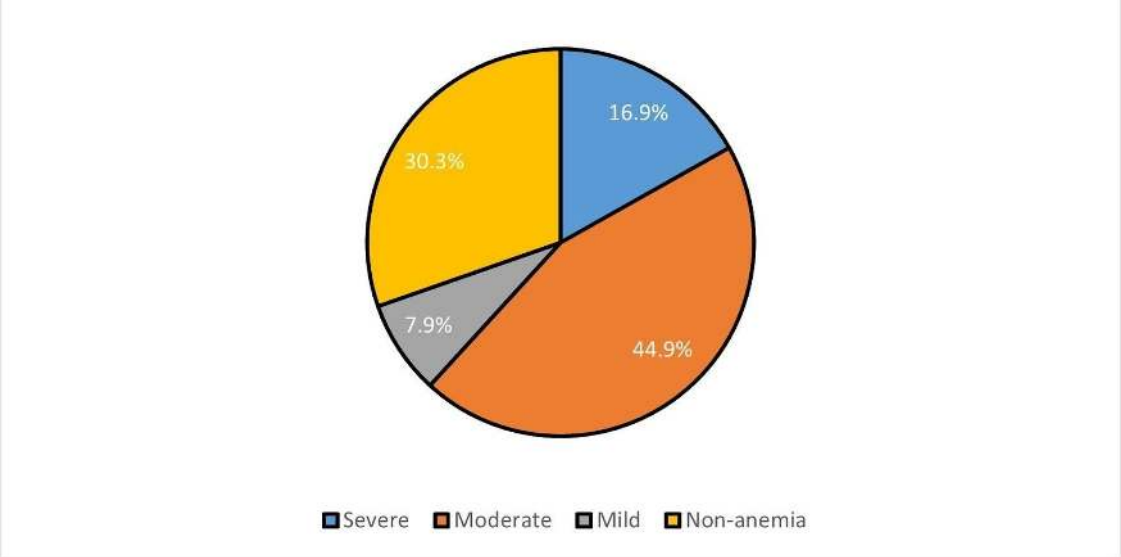

Figure 7.15 Percentage of cases in the selected subjects' population

7.2.2 Selection of the body region of interest

In the beginning, the study was designed to analyze the inside of the hand including fingers and palm. Using palm and fingers as a region of interest is an inexpensive and simple technique especially for developing and in other less developed countries. Other anatomical sites to diagnose anemia include conjunctiva, tongue, and nail bed. [73] In the presence of other diseases that make it difficult to examine conjunctiva, tongue, and nail bed regions, palm and fingers can be used to detect severe anemia. Although, our preliminary data collection phase indicated that including finger images in the study was not feasible due to the fact that each subject had different finger patterns. Some patients, especially those who were elderly, found it difficult to extend their fingers to make the finger creases visible so that a smartphone dermatoscope attachment could capture images of the area. Figure 7:16 is a picture of a 75-year-old subject's finger crease which is an anatomical site called proximal digital. (Figure 7:17) [74] It was particularly challenging to expand this site for elderly and bariatric subjects. As it can be seen from Figure 7:16, due to this problem, it was difficult to obtain high quality less blur images of finger creases.

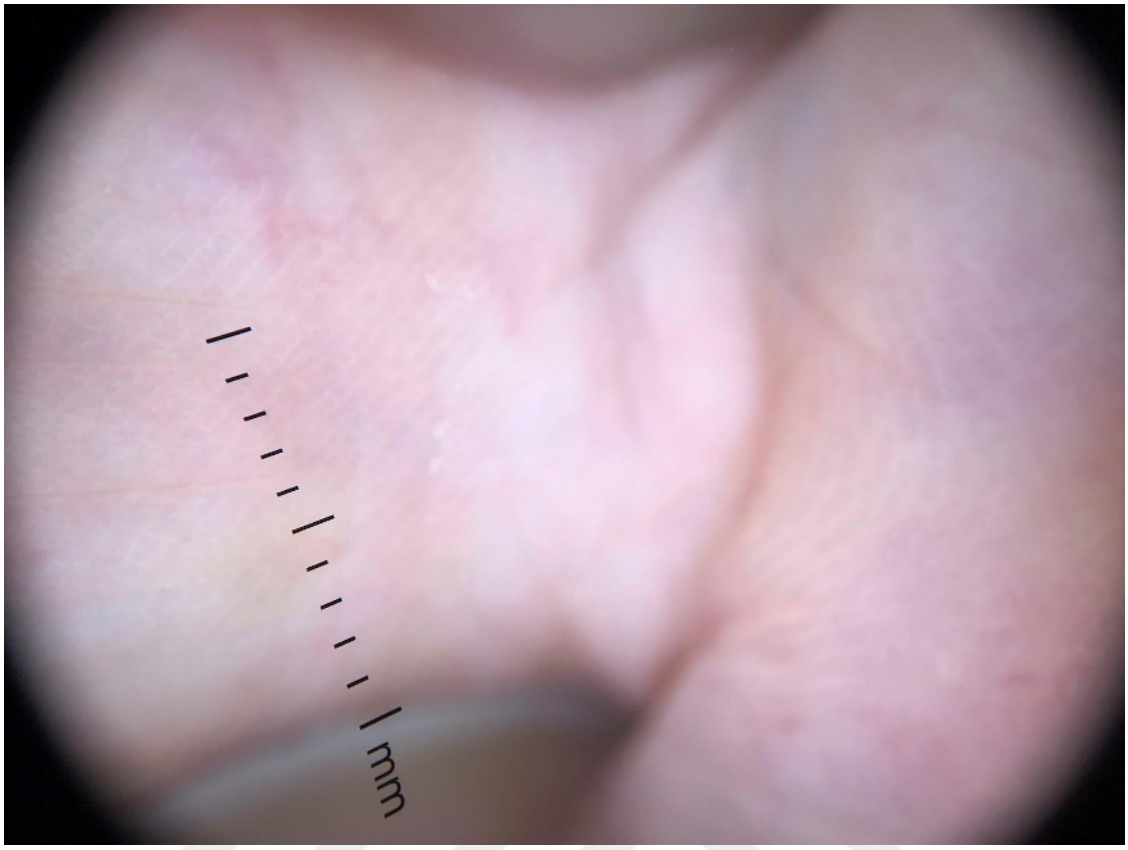

Figure 7.16 Finger crease image of a 75-year-old subject's

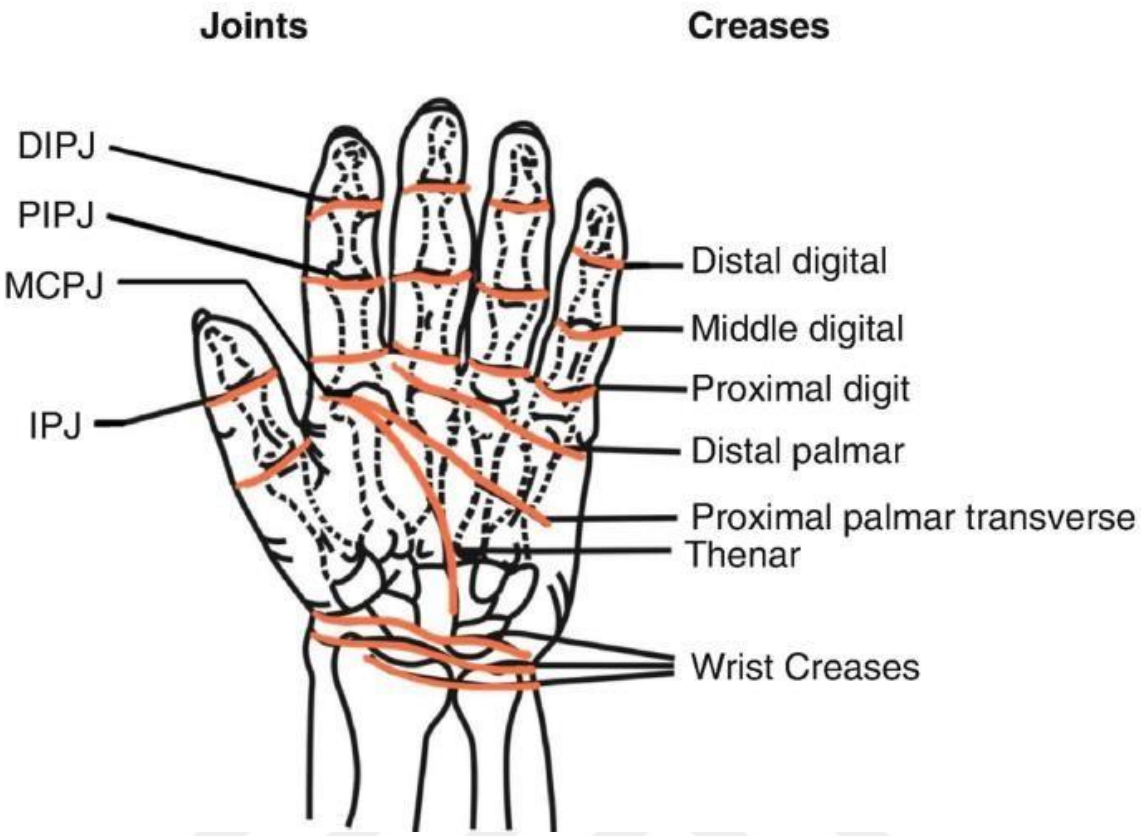

Figure 7.17 Anatomical drawings of the finger and palm creases

Therefore, the palm region is selected as the region of interest and the different parts of the palm from distal palmar, proximal palmar transverse, and thenar (Figure 7:17) of each subject are taken as an image to analyze the color distribution of the palmar creases. Figure 7:18 is a palmar crease image of a subject with 6.1 Hgb value. Color differences between crease and skin are clearly visible.

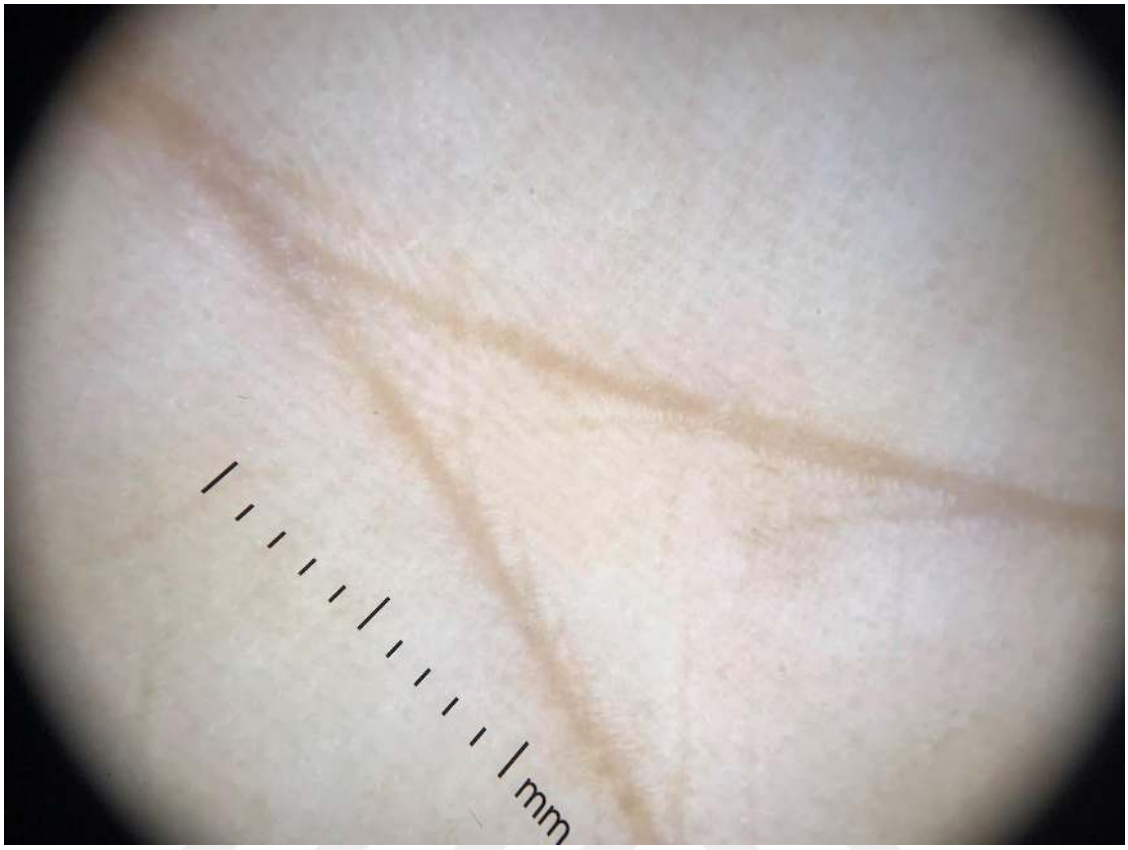

Figure 7.18 Palmar crease image of a subject with 6.1 Hgb value

7.2.3 Selection of the Region of Interest

One of the biggest challenges of choosing palmar crease as a region of interest is changeability and variability. Each person has different palmar crease patterns. Therefore, from individual to individual, the region of interest varies greatly. To overcome this problem, every region of interest is manually selected. The fact that the number of data was not large enabled us to do this. In each image, the best ROI was selected in terms of color variation and resolution quality. The measuring scale position was intentionally avoided as a region of interest area, meaning that it was tried not to select an ROI from the location of the measurement scale. Additionally, the position of each palmar crease pattern in the image changes through different images from the same palm. To avoid this, the same type of ROIs which have the same dimensions were placed in every image manually considering the changing position of the crease. This enables us to understand the color differentiation in the specific palmar crease region (Figure 7:19)

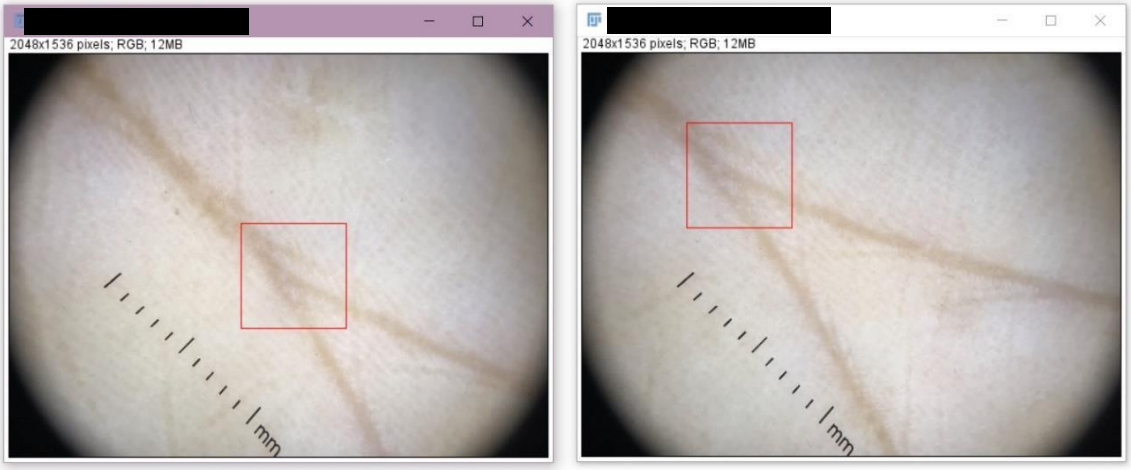

Figure 7.19 Small ROIs in the different images of the same subject

As it was mentioned in the Chapter 4, two different ROIs are selected from each image with Rectangular Selection Tool in the ImageJ software. The one with smaller dimensions is labeled as small due to region of interest, whilst the one with larger dimensions is labeled as big. Although the results have proved that as the area of interest size increases, the observation of the color change decreases. Consequently, the correlation between measured erythema index values and the hemoglobin levels in big regions of interest is less than the correlation between measured erythema index values and the hemoglobin levels in small regions of interest. The big region of interest covers more area in the images; however, it also makes manually addressing the same palmar crease region challenging. As shown in Figure 7:20, while it is easier to define the same palmar crease region in different images with the same small region of interest, the palmar crease that the big region of interest covers, changes from image to image. Therefore, the small region of interest has greater applicability and reliability than the big region of interest.

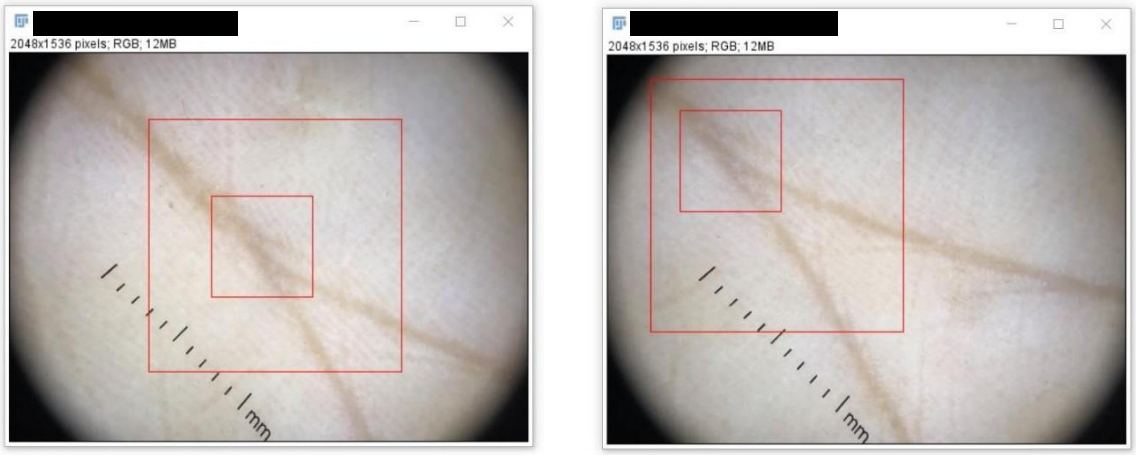

Figure 7.20 Small and Big ROIs in the different images of the same subject

7.3 Statistical Analysis

All statistical tests including regression correlation coefficients, two tailed Student's t tests were performed using GraphPad Prism version 8.0.0 for Windows (GraphPad Software, San Diego, California USA) and Microsoft Excel (Microsoft Corporation, Redmond, WA, USA). The study result is statistically significant ($p < 0.05$).

7.4 Comparison of Hemoglobin levels

As it mentioned in the Chapter 2, a recognition feature called erythema index (EI) which is defined as $EI = \log(R) - \log(G)$ is used to define the color characteristics of the images. In their study, Yamamoto et al., described that the gray value of each pixel within the region of interest has the same correlation with color intensity and thus with erythema index value. The relationship between the measured erythema index values and CBC measured Hgb levels was modeled using linear regression (95% CI n = 88) where the erythema index values defined as independent variables and CBC measured Hgb levels defined as dependent variables. Ordinary least squares regression method was used to describe this correlation and correlation coefficient was found as 0.7477. This indicates that erythema index values and CBC hemoglobin levels had

positive correlation. Residual output of the regression is used to calculate the predicted hemoglobin level. Figure 7:21 shows the correlation between erythema index values and CBC hemoglobin levels with the linear regression graph. Coefficient of Determination, R square value was found as 0.559.

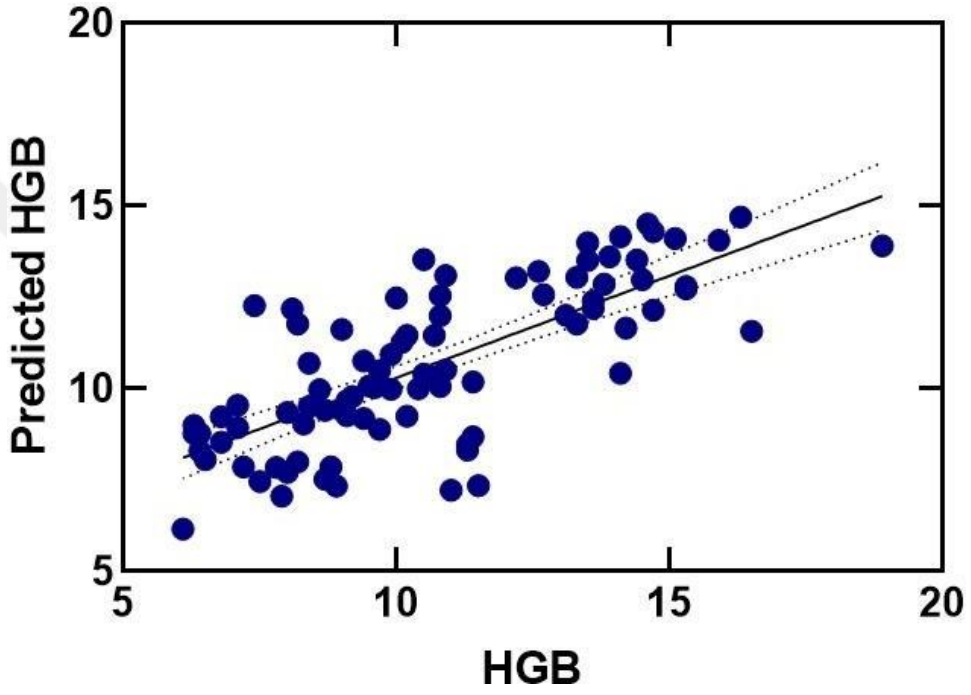

Figure 7.21 Linear regression of the CBC measured HGB levels and predicted HGB values

The difference between the erythema index values and CBC hemoglobin levels is defined as the error. Therefore, absolute mean error was found with the given formula (x) which is the average of all absolute errors between the measured hemoglobin values and the predicted hemoglobin levels. The result for absolute mean error was 1.47 g/dL. Additionally, to compare the results, the Bland - Altman plot is also used. In Figure 7:22, the red lines represent the 95% confidence intervals.

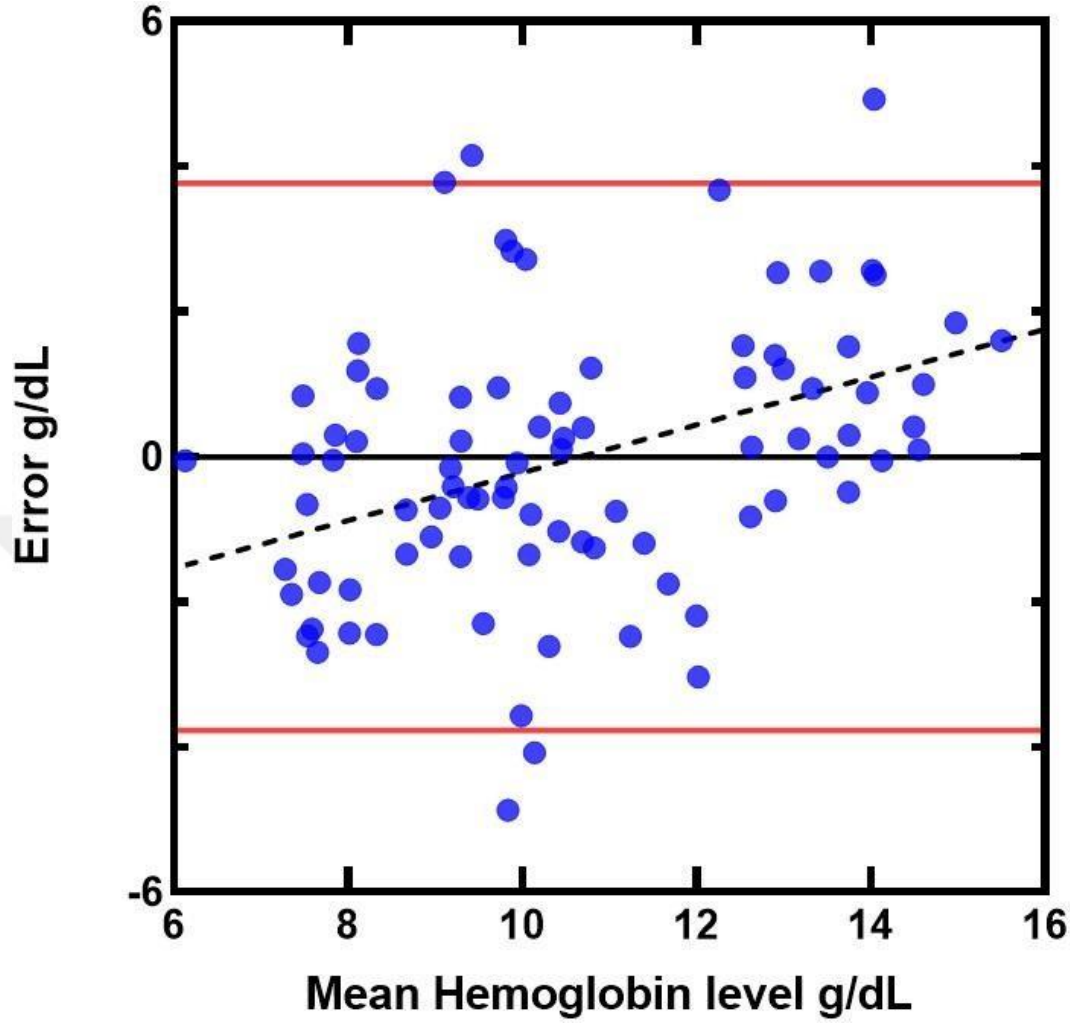

Figure 7.22 Bland - Altman plot of the mean hemoglonin level

Chapter 8: **CONCLUSION**

Anemia, which has multiple causes, such as iron deficiency, chronic blood loss and hemolysis, is a prevalent health problem affecting an estimated two billion people or 30% of the world's population. The ability to measure hemoglobin concentration in anemic patients noninvasively and continuously has significant potential to facilitate hemoglobin monitoring, improve the detection of acute anemia, and avoid the complications, expense and pain associated with invasive blood draws. Although some non-invasive approaches have been developed, they are less accurate than invasive methods as a clinical purpose, resulting in an unmet need for more accurate non-invasive methods.

Therefore, we aimed to develop cost-effective non-invasive self-care anemia evaluation methodology with smartphone- based screening attachments for the first time in the clinic. By examining the color characteristics of the images, we developed an image processing methodology to correlate color characteristics in smartphone images of palm to hemoglobin concentration measured with gold standard hemoglobin measurement system which is CBC test.

The biggest challenge this study encountered was the COVID-19 pandemic. During the data collection phase, the severe acute respiratory syndrome coronavirus 2 (SARS-CoV-2) that causes the new coronavirus illness (COVID-19) appeared. All research activities unrelated to COVID-19 including ours, were suspended as a direct result of the lockdown procedures and the closure of the university research centers including Koc University. The study had to be delayed because of this circumstance. This study was originally planned to be carried out only at Koc University Hospital, Koc University School of Medicine, Istanbul, Turkey. However, due to the emergence of the Covid-19 pandemic, hospitals had restricted the number of patients admitted and the intended number of patients was not reached in the stipulated time when the study was planned. While the pandemic restrictions were still going on, certain hospitals were approached to find out which hospital had the largest patient volume in order to reach the required number of patients. After obtaining the necessary authorizations from both Koc University School of Medicine and Lokman Hekim University School of Medicine, the study was continued at Lokman Hekim University Hospital, Lokman Hekim

University School of Medicine, Ankara, Turkey to expand the patient population. Despite this, we still could not reach the desired number of subjects. Therefore, the main limitation of this study is sample size. Even though the number of subjects enables us to develop a methodology that indicates the correlation between measured hemoglobin values and the predicted hemoglobin levels, data size is not enough to develop a deep convolutional neural network that will make regression and classification prediction. Another challenge was the choosing of the palmar crease as a region of interest due to its changeability and variability. Each person has different palmar crease patterns. To overcome this problem, every region of interest is manually selected. We were able to perform this since the number of data was relatively limited.

According to the results, this method gives significant predicted Hgb values. We observed that our results indicate a correlation between erythema index values and CBC hemoglobin levels. Ordinary least squares regression method was used to describe linear correlation between erythema index values and CBC hemoglobin levels and correlation coefficient was found as 0.7477. This indicates that erythema index values and CBC hemoglobin levels had positive correlation. Residual output of the regression is used to calculate the predicted hemoglobin level and the coefficient of Determination, R square value was found as 0.559. These results prove the linear relationship between color characteristics of digital images and hemoglobin concentration measured in the laboratory.

Nowadays, almost everyone has a mobile phone with a camera equipped. Smartphone approaches to these assessment challenges can potentially address expense and mobility. In addition to having significant computational power, storage and communication capability; smartphones are ubiquitous globally. To date, there are unfortunately only few papers for development of a portable non-invasive methodology using low-cost and smartphone attachments on the diagnosis and follow-up of anemia diseases, especially for precision and personalized patient-oriented medicine. With the proposed methodology, in future cost-effective non-invasive point-of-care system that enables users to make self-care anemia evaluation and screening, which would replace the conventional method of anemia detection by visual observation of palm pallor colors Furthermore, with the developments in cloud technology, the study results can be improved by increasing the number of samples. This can be done with a system that will allow people who have already had blood counts to add photos to the cloud. Sensitivity

can be optimized with a deep learning algorithm, which will be developed based on the correlation found, and values that are much closer to the real hemoglobin results can be obtained. The outcomes of this project can improve health services offered to patients with related diseases / disorders by supporting diagnosis, and early identification of critical situations related to disease severity and therefore decrease the percentage of severe complications of the diseases. These, in turn, are expected to yield significant economic benefits to patients by better planning treatment and avoiding unnecessary treatment schemas. Apart from savings on patient expenses, these savings also encourage health care providers to deliver high-quality, coordinated care at lower costs.

REFERENCES

[1] World Health Organization. 2011. Haemoglobin concentrations for the diagnosis of anaemia and assessment of severity Accessed August 4, 2017 http://www.who.int/vmnis/indicators/haemoglobin.pdf.

[2] Kassebaum NJ, Jasrasaria R, Naghavi M, Wulf SK, Johns N, Lozano R, Regan M, Weatherall D, Chou DP, Eisele TP, Flaxman SR, Pullan RL, Brooker SJ, Murray CJ. A systematic analysis of global anemia burden from 1990 to 2010. Blood. 2014 Jan 30;123(5):615-24. doi: 10.1182/blood-2013-06-508325.

[3] Chaparro, C. M., & Suchdev, P. S. (2019). Anemia epidemiology, pathophysiology, and etiology in low- and middle-income countries. Annals of the New York Academy of Sciences, 1450(1), 15–31. https://doi.org/10.1111/nyas.14092

[4] World Health Organization. 2016. Global Health Observatory data repository: prevalence of anaemia in women Accessed May 2, 2018 http://apps.who.int/gho/data/view.main.GSWCAH28REG.

[5] World Health Organization. 2016. Global Health Observatory data repository: anaemia in children <5 years by region Accessed May 2, 2018 http://apps.who.int/gho/data/view.main.ANEMIACHILDRENv?lang=en.

[6] Patel KV. Epidemiology of anemia in older adults. Semin Hematol. 2008 Oct;45(4):210-7. doi: 10.1053/j.seminhematol.2008.06.006. PMID: 18809090; PMCID: PMC2572827.

[7] Roy CN. Anemia of inflammation. Hematology Am Soc Hematol Educ Program. 2010;2010:276-80. doi: 10.1182/asheducation-2010.1.276. PMID: 21239806.

[8] CDC criteria for anemia in children and childbearing-aged women. Centers for Disease Control (CDC). MMWR Morb Mortal Wkly Rep. 1989 Jun 9; 38(22):400-4, PMID: 2542755

[9] World Health Organization. 2003. Pregnancy, childbirth, postpartum and newborn care: a guide for essential practice Geneva: World Health Organization.

[10] Lutter CK. Iron deficiency in young children in low-income countries and new approaches for its prevention. J Nutr. 2008 Dec;138(12):2523-8. doi: 10.3945/jn.108.095406. PMID: 19022983.

[11] Grantham-McGregor S, Ani C. A review of studies on the effect of iron deficiency on cognitive development in children. J Nutr. 2001 Feb;131(2S-2):649S-666S; discussion 666S-668S. doi: 10.1093/jn/131.2.649S. PMID: 11160596.

[12] WHO: Turning the tide of malnutrition: responding to the challenge of the 21st century 2000 [http://www.who.int/nut/documents/nhd_brochure.pdf] Geneva: WHO (WHO/NHD.007) (accessed Oct 17, 2005)

[13] WHO. Worldwide Prevalence of Anaemia 1993–2005: WHO Global Database on Anaemia. World Health Organization; Geneva, Switzerland: 2008.

[14] WHO Division of Child and Development: Integrated management of childhood illness: conclusions. Bull World Health Org 1997, 75:S119-28

[15] Chalco JP, Huicho L, Alamo C, Carreazo NY, Bada CA. Accuracy of clinical pallor in the diagnosis of anaemia in children: a meta-analysis. BMC Pediatr. 2005 Dec 8;5:46. doi: 10.1186/1471-2431-5-46. PMID: 16336667; PMCID: PMC1325025.

[16] Narla M. The erythrocyte. In: Kenneth K, Marshall A, Lichtman JT, Marcel L, Oliver W, Caligiuri MA, editors. Williams Hematology. 9th ed. USA: McGraw-Hill Education; 2016. pp. 461-915. DOI: 978-0-07-183301-1

[17] Hickner J, Graham DG, Elder NC, Brandt E, Emsermann CB, Dovey S, et al., "Testing process errors and their harms and consequences reported from family medicine practices: a study of the American Academy of Family Physicians National Research Network", Qual Saf Health Care. 2008; 17: 194-200.

[18] Moreno Chulilla JA, Romero Colás MS, Gutiérrez Martín M. Classification of anemia for gastroenterologists. World J Gastroenterol. 2009;15(37):4627-4637. doi:10.3748/wjg.15.4627

[19] Das Makheja K, Kumar Maheshwari B, Arain S, Kumar S, Kumari S, Vikash. The common causes leading to pancytopenia in patients presenting to tertiary care hospital. Pak J Med Sci. 2013;29(5):1108-1111. doi:10.12669/pjms.295.3458

[20] Adamson J.W., & Longo D.L. (2018). Anemia and polycythemia. Jameson J, & Fauci A.S., & Kasper D.L., & Hauser S.L., & Longo D.L., & Loscalzo J(Eds.), Harrison's Principles of Internal Medicine, 20e. McGraw-Hill.

https://accessmedicine.mhmedical.com/content.aspx?bookid=2129&sectionid=192014145

[21] Prchal JT. Clinical Manifestations and Classification of Erythrocyte Disorders. In: Kaushansky K, Prchal JT, Burns LJ, Lichtman MA, Levi M, Linch DC. eds. Williams Hematology, 10e. McGraw-Hill; Accessed April 11, 2021. https://accessmedicine.mhmedical.com/content.aspx?bookid=2962&sectionid=252526776

[22] Tefferi A. Anemia in adults: a contemporary approach to diagnosis. Mayo Clin Proc. 2003 Oct;78(10):1274-80. doi: 10.4065/78.10.1274. PMID: 14531486.

[23] Tefferi A. Practical algorithms in anemia diagnosis. Mayo Clin Proc. 2004 Jul;79(7):955-6. doi: 10.4065/79.7.955. PMID: 15244401.

[24] Guyatt GH, Oxman AD, Ali M, Willan A, McIlroy W, Patterson C. Laboratory diagnosis of iron-deficiency anemia: an overview. J Gen Intern Med. 1992 Mar-Apr;7(2):145-53. doi: 10.1007/BF02598003. Erratum in: J Gen Intern Med 1992 Jul-Aug;7(4):423. PMID: 1487761.

[25] Tefferi A, Hanson CA, Inwards DJ. How to interpret and pursue an abnormal complete blood cell count in adults. Mayo Clin Proc. 2005;80(7):923-936. doi:10.4065/80.7.923

[26] Nagao T, Hirokawa M. Diagnosis and treatment of macrocytic anemias in adults. J Gen Fam Med. 2017;18(5):200-204. Published 2017 Apr 13. doi:10.1002/jgf2.31

[27] Nidhi Raval, Rahul Maheshwari, Dnyaneshwar Kalyane, Susanne R. Youngren-Ortiz, Mahavir B. Chougule, Rakesh K. Tekade, Chapter 10 - Importance of Physicochemical Characterization of Nanoparticles in Pharmaceutical Product Development, In Advances in Pharmaceutical Product Development and Research, Basic Fundamentals of Drug Delivery, Academic Press, 2019, Pages 369-400, https://doi.org/10.1016/B978-0-12-817909-3.00010-8.

[28] Phillips J, Henderson AC. Hemolytic Anemia: Evaluation and Differential Diagnosis. Am Fam Physician. 2018 Sep 15;98(6):354-361. PMID: 30215915.

[29] E.D. Yenilmez, A. Tuli, Laboratory approach to anemia: current topics in anemia, Jesmine Khan, IntechOpen, (2017), 10.5772/intechopen.70359, https://www.intechopen.com/books/current-topics-in-anemia/laboratory-approach-to-anemia

[30] Wittenmeier E, Bellosevich S, Mauff S, Schmidtmann I, Eli M, Pestel G, Noppens RR. Comparison of the gold standard of hemoglobin measurement with the clinical standard (BGA) and noninvasive hemoglobin measurement (SpHb) in small children: a prospective diagnostic observational study. Paediatr Anaesth. 2015 Oct;25(10):1046-53. doi: 10.1111/pan.12683. Epub 2015 Jul 14. PMID: 26179143.

[31] Adamson JW, Longo DL. Anemia and Polycythemia. In: Jameson J, Fauci AS, Kasper DL, Hauser SL, Longo DL, Loscalzo J. eds. Harrison's Principles of Internal Medicine, 20e. McGraw-Hill; Accessed April 14, 2021. https://accessmedicine.mhmedical.com/content.aspx?bookid=2129&sectionid=192014145

[32] Cho J, Oh J, Lee SG, Lee YH, Song J, Kim JH. Performance Evaluation of Body Fluid Cellular Analysis Using the Beckman Coulter UniCel DxH 800, Sysmex XN-350, and UF-5000 Automated Cellular Analyzers. Ann Lab Med. 2020 Mar;40(2):122-130. doi: 10.3343/alm.2020.40.2.122. PMID: 31650728; PMCID: PMC6822009.

[33] Gulati G, Song J, Florea AD, Gong J. Purpose and criteria for blood smear scan, blood smear examination, and blood smear review. Ann Lab Med. 2013 Jan;33(1):1-7. doi: 10.3343/alm.2013.33.1.1. Epub 2012 Dec 17. PMID: 23301216; PMCID: PMC3535191.

[34] Roychowdhury, S., Hage, P., & Vasquez, J. (2017). Azure-Based Smart Monitoring System for Anemia-Like Pallor. Future Internet, 9(3), 39. doi: 10.3390/fi9030039

[35] (2) Sanchis-Gomar, F., Cortell-Ballester, J., Pareja-Galeano, H., Banfi, G., & Lippi, G. (2012). Hemoglobin Point-of-Care Testing. Journal Of Laboratory Automation, 18(3), 198-205. doi: 10.1177/2211068212457560

[36] Gehring, H., Hornberger, C., Dibbelt, L., Roth-Isigkeit, A., Gerlach, K., Schumacher, J., & Schmucker, P. (2002). Accuracy of point-of-care-testing (POCT) for determining hemoglobin concentrations. Acta Anaesthesiologica Scandinavica, 46(8), 980-986. doi: 10.1034/j.1399-6576.2002.460809.x

[37] HemoCue® Hb 801 Operating Manual. Retrieved 31 March 2021, from https://www.hemocue.us/wp-content/uploads/2020/07/HemoCue_Hb_801_System_Operating_Manual.pdf

[38] Lardi, A. M.; Hirst, C.; Mortimer, A. J.; McCollum, C. N. Evaluation of the HemoCue for Measuring Intra-operative Haemoglobin Concentrations: A Comparison with the Coulter Max-M. Anaesthesia 1998, 53(4), 349–352.

[39] Paddle, J. J. Evaluation of the Haemoglobin Colour Scale and Comparison with the HemoCue Haemoglobin Assay. Bull. World Health Organ. 2002, 80(10), 813–816.

[40] Morris, L. D.; Osei-Bimpong, A.; McKeown, D.; Roper, D.; Lewis, S. M. Evaluation of the Utility of the HemoCue 301 Haemoglobinometer for Blood Donor Screening. Vox Sang. 2007, 93(1), 64–69.

[41] Gehring, H., Hornberger, C., Dibbelt, L., Rothsigkeit, A., Gerlach, K., Schumacher, J., & Schmucker, P. (2002). Accuracy of point-of-care-testing (POCT) for determining hemoglobin concentrations. Acta anaesthesiologica Scandinavica, 46(8), 980–986. https://doi.org/10.1034/j.1399-6576.2002.460809.x

[42] Yamamoto, T., Takiwaki, H., Arase, S., & Ohshima, H. (2007). Derivation and clinical application of special imaging by means of digital cameras and image j freeware for quantification of erythema and pigmentation. Skin Research and Technology, 14, 26-34. doi:10.1111/j.1600-0846.2007.00256.x

[43] Kumar, R.; Ranganathan, H. Noninvasive sensor technology for total hemoglobin measurement in blood. J. Ind. Intell. Inf. 2013, 1, 243–246

[44] McMurdy JW, Jay GD, Suner S, Crawford G. Noninvasive optical, electrical, and acoustic methods of total hemoglobin determination. Clin Chem. 2008 Feb;54(2):264-72. doi: 10.1373/clinchem.2007.093948. Epub 2007 Dec 10. PMID: 18070818.

[45] Rossi-Bernardi L, Perella M, Luzzana M, Samaja M, Raffaele I. Simultaneous determination of hemoglobin derivatives, oxygen content, oxygen capacity, and oxygen saturation in 10 microliters of whole blood. Clin Chem. 1977 Jul;23(7):1215-25. PMID: 872367.

[46] Farmer J. Blood oxygen measurement. In: Webster JG, editor. Design of Pulse Oximeters. Bristol: Institute of Physics; 1997. pp. 21–39.

[47] Aldrich TK, Moosikasuwan M, Shah SD, Deshpande KS. Length-Normalized Pulse Photoplethysmography: A Noninvasive Method to Measure Blood

Hemoglobin, Bronx, NY. Annals of Biomedical Engineering. 2002;30(10):1291-1298. doi:10.1114/1.1527046

[48] Kim O, McMurdy J, Jay G, Lines C, Crawford G, Alber M. Combined reflectance spectroscopy and stochastic modeling approach for noninvasive hemoglobin determination via palpebral conjunctiva. Physiol Rep. 2014;2(1):e00192. Published 2014 Jan 8. doi:10.1002/phy2.192

[49] Zhang C, Cheng G, Edwards P, Zhou MD, Zheng S, Liu Z. G-Fresnel smartphone spectrometer. Lab Chip. 2016 Jan 21;16(2):246-50. doi: 10.1039/c5lc01226k. PMID: 26645747

[50] Wang, E. J., Li, W., Hawkins, D., Gernsheimer, T., Norby-Slycord, C., & Patel, S. N. (2016). HemaApp. Proceedings of the 2016 ACM International Joint Conference on Pervasive and Ubiquitous Computing. doi:10.1145/2971648.2971653

[51] Hasan, M. K., Haque, M., Sakib, N., Love, R., & Ahamed, S. I. (2018). Smartphone-based human Hemoglobin Level Measurement Analyzing pixel intensity of a fingertip video on different color spaces. Smart Health, 5-6, 26-39. doi:10.1016/j.smhl.2017.11.003

[52] Anggraeni, M. D., & Fatoni, A. (2017). Non-invasive self-care anemia detection during pregnancy using a smartphone camera. IOP Conference Series: Materials Science and Engineering, 172, 012030. doi:10.1088/1757-899x/172/1/012030

[53] Aldrich TK, Moosikasuwan M, Shah SD, Deshpande KS. Length-Normalized Pulse Photoplethysmography: A Noninvasive Method to Measure Blood Hemoglobin, Bronx, NY. Annals of Biomedical Engineering. 2002;30(10):1291-1298. doi:10.1114/1.1527046

[54] De Haan, K., Ceylan Koydemir, H., Rivenson, Y., Tseng, D., Van Dyne, E., Bakic, L., . . . Ozcan, A. (2020). Automated screening of sickle cells using a smartphone-based microscope and deep learning. Npj Digital Medicine, 3(1). doi:10.1038/s41746-020-0282-y

[55] De Greef, L., Goel, M., Seo, M. J., Larson, E. C., Stout, J. W., Taylor, J. A., & Patel, S. N. (2014). Bilicam. Proceedings of the 2014 ACM International Joint Conference on Pervasive and Ubiquitous Computing: Adjunct Publication. doi:10.1145/2638728.2638803

[56] Kalantri A, Karambelkar M, Joshi R, Kalantri S, Jajoo U. Accuracy and reliability of pallor for detecting anaemia: a hospital-based diagnostic accuracy study. PLoS One. 2010 Jan 1;5(1):e8545. doi: 10.1371/journal.pone.0008545. PMID: 20049324; PMCID: PMC2797134.

[57] Mannino, R.G., Myers, D.R., Tyburski, E.A. et al. Smartphone app for non-invasive detection of anemia using only patient-sourced photos. Nat Commun 9, 4924 (2018). https://doi.org/10.1038/s41467-018-07262-2

[58] Barker SJ, Badal JJ. The measurement of dyshemoglobins and total hemoglobin by pulse oximetry. Curr Opin Anaesthesiol. 2008 Dec;21(6):805-10. doi: 10.1097/ACO.0b013e328316bb6f. PMID: 18997533.

[59] Pinto M, Barjas-Castro ML, Nascimento S, Falconi MA, Zulli R, Castro V. The new noninvasive occlusion spectroscopy hemoglobin measurement method: a reliable and easy anemia screening test for blood donors. Transfusion. 2013 Apr;53(4):766-9. doi: 10.1111/j.1537-2995.2012.03784.x. Epub 2012 Jul 15. PMID: 22803617.

[60] Selim Suner, Gregory Crawford, John McMurdy, Gregory Jay, Non-Invasive Determination of Hemoglobin by Digital Photography of Palpebral Conjunctiva, The Journal of Emergency Medicine,Volume 33, Issue 2, 2007,Pages 105-111, ISSN 0736-4679, https://doi.org/10.1016/j.jemermed.2007.02.011

[61] Collings S, Thompson O, Hirst E, Goossens L, George A, Weinkove R. Non-Invasive Detection of Anaemia Using Digital Photographs of the Conjunctiva. PLoS One. 2016 Apr 12;11(4):e0153286. doi: 10.1371/journal.pone.0153286. PMID: 27070544; PMCID: PMC4829242.

[62] Yamamoto, T., Takiwaki, H., Arase, S., & Ohshima, H. (2007). Derivation and clinical application of special imaging by means of digital cameras and image j freeware for quantification of erythema and pigmentation. Skin Research and Technology, 14, 26-34. doi:10.1111/j.1600-0846.2007.00256.x

[63] Mitani, A., Huang, A., Venugopalan, S. et al. Detection of anaemia from retinal fundus images via deep learning. Nat Biomed Eng 4, 18–27 (2020). https://doi.org/10.1038/s41551-019-0487-z

[64] Chen YM, Miaou SG, Bian H. Examining palpebral conjunctiva for anemia assessment with image processing methods. Comput Methods Programs

Biomed. 2016 Dec;137:125-135. doi: 10.1016/j.cmpb.2016.08.025. Epub 2016 Sep 7. PMID: 28110719.

[65] An R, Huang Y, Man Y, Valentine RW, Kucukal E, Goreke U, Sekyonda Z, Piccone C, Owusu-Ansah A, Ahuja S, Little JA, Gurkan UA. Emerging point-of-care technologies for anemia detection. Lab Chip. 2021 May 18;21(10):1843-1865. doi: 10.1039/d0lc01235a. PMID: 33881041; PMCID: PMC8875318.

[66] Strobach RS, Anderson SK, Doll DC, Ringenberg QS. The value of the physical examination in the diagnosis of anemia. Correlation of the physical findings and the hemoglobin concentration. Arch Intern Med. 1988 Apr;148(4):831-2. PMID: 3355303

[67] Wan S, Parrish JA, Jaenicke KF. Quantitative evaluation of ultraviolet induced erythema. Photochem Photobiol. 1983 Jun;37(6):643-8. doi: 10.1111/j.1751-1097.1983.tb04533.x. PMID: 6611670.

[68] Feather JW, Ellis DJ, Leslie G. A portable reflectometer for the rapid quantification of cutaneous haemoglobin and melanin. Phys Med Biol. 1988 Jun;33(6):711-22. doi: 10.1088/0031-9155/33/6/005. PMID: 3406055.

[69] Fullerton A, Fischer T, Lahti A, Wilhelm KP, Takiwaki H, Serup J. Guidelines for measurement of skin colour and erythema. A report from the Standardization Group of the European Society of Contact Dermatitis. Contact Dermatitis. 1996;35(1):1-10. doi:10.1111/j.1600-0536.1996.tb02258.x

[70] Takiwaki H, Shirai S, Kanno Y, Watanabe Y, Arase S. Quantification of erythema and pigmentation using a videomicroscope and a computer. Br J Dermatol. 1994;131(1):85-92. doi:10.1111/j.1365-2133.1994.tb08462.x

[71] Schneider, C. A., Rasband, W. S., & Eliceiri, K. W. (2012). NIH Image to ImageJ: 25 years of image analysis. Nature Methods, 9(7), 671–675. doi:10.1038/nmeth.2089.

[72] Sohrabi, C., Alsafi, Z., O'Neill, N., Khan, M., Kerwan, A., Al-Jabir, A., Iosifidis, C., & Agha, R. (2020). World Health Organization declares global emergency: A review of the 2019 novel coronavirus (COVID-19). International journal of surgery (London, England), 76, 71–76. https://doi.org/10.1016/j.ijsu.2020.02.034

[73] Santra, G. (2015). Usefulness of examination of palmar creases for assessing severity of anemia in Indian perspective: A study from a tertiary care center. International Journal of Medicine and Public Health, 5(2), 169.

[74] Wakure, A., Omkumar, A., Tharayil, J. (2020). Clinical Examination of the Hand and Fingers (Basic and Surface Anatomy) with Special Tests. In: Iyer, K., Khan, W. (eds) Orthopedics of the Upper and Lower Limb. Springer, Cham. https://doi.org/10.1007/978-3-030-43286-7_8